Accepted Manuscript

Design and synthesis of BPR1K653 derivatives targeting the back pocket of Aurora kinases for selective isoform inhibition

Yi-Yu Ke, Chun-Ping Chang, Wen-Hsing Lin, Chia-Hua Tsai, I-Chen Chiu, Wan-Ping Wang, Pei-Chen Wang, Pei-Yi Chen, Wen-Hsin Lin, Chun-Feng Chang, Po-Chu Kuo, Jen-Shin Song, Chuan Shih, Hsing-Pang Hsieh, Ya-Hui Chi

PII: S0223-5234(18)30307-6

DOI: 10.1016/j.ejmech.2018.03.064

Reference: EJMECH 10329

To appear in: *European Journal of Medicinal Chemistry*

Received Date: 18 August 2017

Revised Date: 14 March 2018

Accepted Date: 21 March 2018

Please cite this article as: Y.-Y. Ke, C.-P. Chang, W.-H. Lin, C.-H. Tsai, I.-C. Chiu, W.-P. Wang, P.-C. Wang, P.-Y. Chen, W.-H. Lin, C.-F. Chang, P.-C. Kuo, J.-S. Song, C. Shih, H.-P. Hsieh, Y.-H. Chi, Design and synthesis of BPR1K653 derivatives targeting the back pocket of Aurora kinases for selective isoform inhibition, *European Journal of Medicinal Chemistry* (2018), doi: 10.1016/j.ejmech.2018.03.064.

Design and synthesis of BPR1K653 derivatives targeting the back pocket of Aurora kinases for selective isoform inhibition

Yi-Yu Ke[a, 1], Chun-Ping Chang[a, 1], Wen-Hsing Lin[a], Chia-Hua Tsai[a], I-Chen Chiu[a], Wan-Ping Wang[a], Pei-Chen Wang[a], Pei-Yi Chen[a], Wen-Hsin Lin[a], Chun-Feng Chang[a], Po-Chu Kuo, Jen-Shin Song, Chuan Shih[a], Hsing-Pang Hsieh[a,b**], Ya-Hui Chi[a,c*]

[a] *Institute of Biotechnology and Pharmaceutical Research, National Health Research Institutes, Zhunan 35053, Taiwan, R. O. C.*

[b] *Department of Chemistry, National Tsing Hua University, Hsinchu 30013, Taiwan, ROC.*

[c] *Graduate Institute of Basic Medical Science, China Medical University, Taichung 40402, Taiwan, R. O. C.*

** Corresponding author.

* Corresponding author.

E-mail addresses: ychi@nhri.org.tw (Y.H. Chi), hphsieh@nhri.org.tw (H.P. Hsieh)

[1] These authors are equal contributors.

Abbreviations. SAC, spindle assembly checkpoint; CPC, chromosomal passenger complex; pHH3Ser10, phosphorylation on serine 10 of histone H3; MI, mitotic index.

Highlights

- 25 new furanopyrimidine analogs were designed and synthesized.
- The designed compounds were evaluated for Aurora-A and Aurora-B inhibition activity.
- Derivatization on the phenylurea modulates isoform-selective kinase inhibition.
- Molecular docking studies were performed.

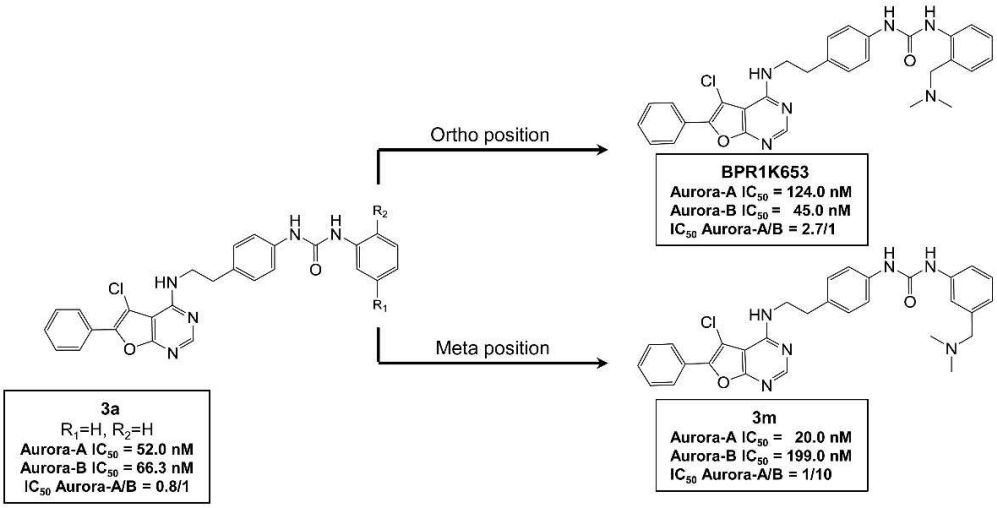

Graphical abstract

Abstract

Twenty five novel chemical analogs of the previously reported Aurora kinase inhibitor **BPR1K653** (1-(4-(2-((5-chloro-6-phenylfuro[2,3-d]pyrimidin-4-yl)amino)ethyl)phenyl)-3-(2-((dimethylamino)methyl)phenyl)urea) have been designed, synthesized, and evaluated by Aurora-A and Aurora-B enzymatic kinase activity assays. Similar to **BPR1K653**, analogs **3b**-**3h** bear alkyl or tertiary amino group at the ortho position of the phenylurea, and showed equal or better inhibition activity for Aurora-B over Aurora-A. Conversely, preferential Aurora-A inhibition activity was observed when the same functional group was moved to the meta position of the phenylurea. Compounds **3m** and **3n**, both of which harbor a tertiary amino group at the meta position of the phenylurea, showed 10-16 fold inhibition selectivity for Aurora-A over Aurora-B. The *in vitro* kinase inhibition results were verified by Western blot analysis, and indicated that compounds **3m** and **3n** were more than 75-fold superior in inhibiting T-loop autophosphorylation of Aurora-A (Thr288), compared to Aurora-B (Thr232) in HCT116 colon carcinoma cells. The computational docking analysis suggested that the tertiary amine at the meta position of the phenylurea formed a more stable interaction with residues in the back pocket of Aurora-A than in Aurora-B, a possible explanation for the observed discrepancy in the selectivity. These results support an alternative small molecule design strategy targeting

the back pocket of Aurora kinases for selective isoform inhibition.

Key words: Aurora kinase inhibitor, anticancer agents, docking study

Introduction

Aurora kinases are serine/threonine kinases which regulate mitotic progression, centrosome maturation, and spindle assembly [1, 2]. Overexpression of Aurora kinases has been associated with increased tumor progression, and thus they are appealing targets for the development of anti-cancer therapies [3-7].

Despite similarities in protein sequence, the sub-cellular localization, expression patterns, timing, and activity of Aurora-A are markedly different to Auroras -B and -C [1]. Aurora-A primarily localizes to centrosomes and mitotic spindles where it regulates centrosome duplication, centrosome maturation, and mitotic spindle formation. Disruption of Aurora-A kinase activity arrests cells in the G2/M stage of the cell cycle, thereby activating the spindle assembly checkpoint (SAC) and thus growth inhibition [8, 9]. On the other hand, Aurora-B is part of the chromosomal passenger complex (CPC), a hetero-tetrameric complex composed of Aurora-B, inner centromere protein (INCENP), Borealin and Survivin [10, 11]. In prometaphase, the CPC localizes at the centromeric region of the chromosome, monitoring proper attachment of microtubules emanating from opposite poles of the cell, activating SAC, as well as promoting chromosome congression to the metaphase plate [12-14]. Inhibiting the kinase activity of Aurora-B or depleting INCENP results in dephosphorylation of histone H3 on serine 10 and override of SAC

[15, 16], leading to premature decondensation of the chromatin, an increased degree of polyploidy, cell senescence, and apoptosis [17, 18].

Aurora -A or -B selective and pan-aurora inhibitors have demonstrated different preclinical and clinical therapeutic efficacies [2, 19-23]. For example, clinical trials for a pan-Aurora inhibitor VX-680 (developed by Vertex) were halted at phase II for toxicity reasons (one case of heart failure) [6, 24]. VX-689, a newer version of VX-680 which showed higher Aurora-A selectivity, has entered a phase I clinical trial [25]. MLN8237, developed by Millennium, exhibited better Aurora-A selectivity over MLN8054. A clinical trial of MLN8054 was terminated due to severe neutropenia, while MLN8237 has entered phase III clinical trials [25, 26]. These clinical observations suggest that development of Aurora-A selective compounds may be beneficial for the treatment of solid tumors due to the reduced toxicity to cells in the myeloid lineage. On the other hand, higher response rates against hematologic malignancies have been observed in clinical trials for drugs with better Aurora-B inhibition efficacy [27].

We previously discovered a pan-Aurora kinase inhibitor named **BPR1K653** (i.e. 1-(4-(2-((5-chloro-6-phenylfuro[2,3-d]pyrimidin-4-yl)amino)ethyl)phenyl)-3-(2-((dimeth ylamino)methyl)phenyl)urea, Fig. 1) which showed potency against various tumors independent of the expression of MDR1 (multidrug resistance protein 1) [28]. By synthesis

of a series of furanopyrimidine analogs followed by activity validation using enzymatic and cellular assays, and molecular docking, these small molecules were determined to interact differently with residues in the back pocket of Aurora-A and Aurora-B, accounting for their selective inhibition activities.

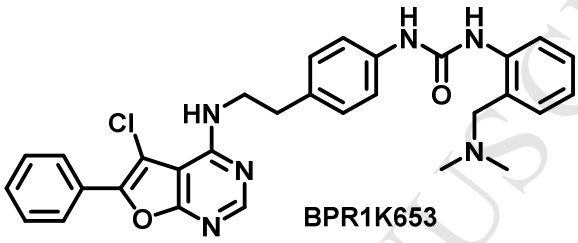

Fig. 1. Molecular structure of **BPR1K653**, a pan-Aurora kinase inhibitor.

2. Results and Discussion

2.1. Chemistry

The preparation of compounds **3a-3y** bearing modifications on the urea side chain was achieved by modifying strategies in previous reports (Scheme1) [29, 30]. S_NAr reaction of dichlorofuranopyrimidine **1** [30] with 4-(2-aminoethyl)aniline in ethanol gave the desired intermediate compound **2**, which was converted to the corresponding urea compound **3a-3y** by reaction with various isocyanates or carbamates, respectively.

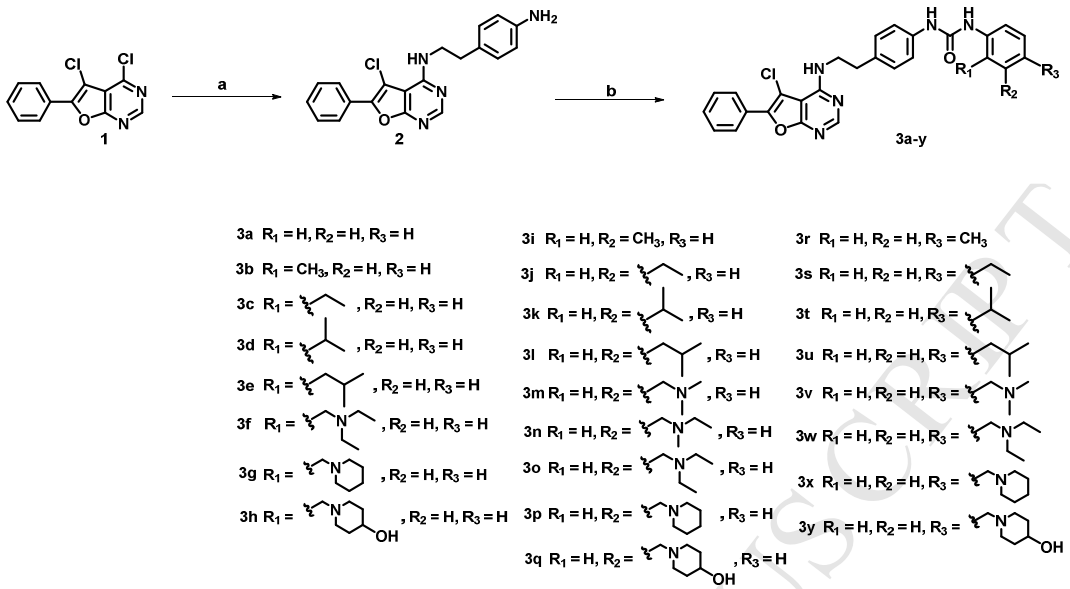

Scheme 1. Synthesis of compounds **3a-3y**. Reaction conditions and reagents: (a) 4-(2-aminoethyl)aniline, EtOH, reflux, 1 h, 86%; (b) (i) various isocyanates, CH_2Cl_2, rt, 4 h, 34-66%; or (ii) various carbamates, Et_3N, 1,4-dioxane, 120 ℃, 8 h, 20-64%.

2.2. Biological evaluation

2.2.1. Aurora inhibition activity of the compounds

Enzymatic inhibition activities of compounds **3a-3y** to Aurora-A and Aurora-B were evaluated by ATP consumption assays. Table 1 summarizes the structure-activity relationship (SAR) results for different substituents at the ortho, meta or para position of the phenylurea. The results indicated that removing all substitutions on the phenylurea (i.e. compound **3a**) resulted in near equal inhibition activity to Aurora-A and Aurora-B. On the other hand, replacing the *N*,*N*-dimethyl tertiary amino group of **BPR1K653** (Aurora-A IC_{50} = 124.0 nM; Aurora-B IC_{50} = 45.0 nM) with an isobutyl group (compound **3e**)

dramatically reduced inhibition activity of Aurora-A and Aurora-B (Aurora-A IC_{50} = 3000.0 nM; Aurora-B IC_{50} = 700.3 nM). This effect was less significant when the number of carbon atoms in R1 is less than four (i.e. compounds **3b-3d**). Compound **3h**, which contains a 4-hydroxypiperidinyl group at the ortho position of the phenylurea showed increased Aurora-B inhibition activity compared to **3f** and **3g**, implying that improved hydrophilicity may be beneficial for the interaction between the functional groups and residues in the back pocket of Aurora-B.

Relocation of the isobutyl group of **3e** from the ortho position to the meta position of phenylurea gave **3l**, which was a much more potent inhibitor of Aurora-A than Aurora-B (Aurora-A IC_{50} = 247.0 nM; Aurora-B IC_{50} >10000 nM). Our results for 3**i**-3**l** suggested that Aurora-B inhibition potency drastically decreased with increased number of carbons at the meta position of the phenylurea. The Aurora-A inhibition potency was increased 12 fold in **3m** (Aurora-A IC_{50} = 20.0 nM), which bears a *N*,*N*-dimethyl tertiary amino group at the meta position of phenylurea (Table 1), compared to **3l** (Aurora-A IC_{50} = 247.0 nM), which contains an isobutyl group. Similar Aurora-A inhibition potency was observed in **3n** (Aurora-A IC_{50} = 9.0 nM) and **3o** (Aurora-A IC_{50} = 21.5 nM). However, further extension of the carbon chain on the tertiary amino group (**3p**-**3q**) reduced the Aurora-A inhibition potency compared to **3o**.

We also synthesized compounds bearing the same alkyl and tertiary amino groups at the para position of the phenylurea, and measured their inhibition activity to Aurora-A and Aurora-B. As indicated in Table 1, addition of tertiary amino groups at the para position of phenylurea (i.e. compounds **3v**-**3y**) did not improve inhibition selectivity to Aurora-A compared to the meta derivatives (i.e. compounds **3m**-**3q**), or the inhibition selectivity to Aurora-B compared to the ortho derivatives (i.e. compounds **3f**-**3h** and **BPR1K653**).

Table 1. Structure and enzymatic evaluation of the prepared compounds.

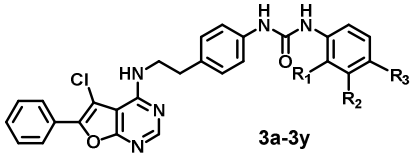

3a-3y

Compound	R_1	R_2	R_3	Aurora-A IC_{50}[a] (nM)	Aurora-B IC_{50}[b] (nM)
BPR1K653		H	H	124.0	45.0
3a	H	H	H	52.0	66.3
3b	CH_3	H	H	83.2	60.2
3c		H	H	178.0	66.2
3d		H	H	525.0	335.9
3e		H	H	>1000[c]	700.3
3f		H	H	461.9	526.1
3g		H	H	198.0	121.6
3h	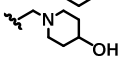	H	H	228.0	78.9
3i	H	CH_3	H	52.6	74.9
3j	H		H	66.3	86.1
3k	H		H	233.0	657.1
3l	H		H	247.0	>1000[c]
3m	H		H	20.0	199.0
3n	H		H	9.0	140.4
3o	H		H	21.5	121.5
3p	H		H	90.2	102.3
3q	H	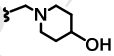	H	67.8	83.6
3r	H	H	CH_3	55.5	73.3
3s	H	H		139.3	443.0
3t	H	H		>1000[c]	>1000[c]
3u	H	H		>1000[c]	>1000[c]
3v	H	H		98.3	455.5
3w	H	H		232.0	835.2
3x	H	H		451.0	975.9
3y	H	H	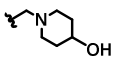	150.0	352.5

[a] IC_{50} values are calculated from duplicated ATP consumption assays of 9 titration points.

[b] IC_{50} values are calculated from duplicated ATP consumption assays of 7 titration points.

[c] Less than 50% inhibition at 1000 nM.

2.2.2 Aurora-A and Aurora-B inhibitory activity of the synthesized compounds in cells

Autophosphorylation of Aurora kinases has been found to be indispensable for their activation [31, 32]. To test the inhibition selectivity of the synthesized compounds in cells, we profiled phosphorylated Aurora-A (Thr288), Aurora-B (Thr232) and Aurora-C (Thr198) using Western blotting. Compounds **3m** and **3n** were found to be more potent inhibitors of autophosphorylation of Aurora-A than Aurora-B, while compounds **3h** and **BPR1K653** favored Aurora-B inhibition (Fig. 2 and Table 2). These data are consistent with our observations made in the enzymatic kinase activity assays (Table 1). We noted that the inhibition potency of compounds **3m** and **3n** to Aurora-B (Thr232) phosphorylation is much less than compound **3h** in HCT116 cells (Table 2) though the cell-free enzymatic inhibition activity is only 2-fold less (Table 1). This discrepancy may be due to preference of compounds **3m** and **3n** to interact with Aurora-A than Aurora-B in cells which preserve authentic complex interactions.

Inhibiting the kinase activity of either Aurora-A or Aurora-B can halt cell proliferation, though the mechanisms of action are different [1]. In addition, inhibiting the kinase activity of Aurora-B has been shown to be more efficient than Aurora-A for cell growth arrest and apoptosis [33-37]. That is probably why compounds **3a**, **3h**, **3m** and **3n**

all inhibited proliferation of HCT116 human colon carcinoma cells at the sub-micro molar range (Table 2), although they possess various inhibition activities against Aurora isoforms. BPR1K653 showed the best anti-proliferation activity, perhaps because it is also the most potent Aurora-B inhibitor amongst the analyzed compounds (Tables 1-2). To determine if the compounds are cytotoxic to non-cancerous cells, we tested proliferation inhibition of the compounds to Detroit 551 (normal human skin fibroblasts). The inhibition concentrations of compounds **3a**, **3h**, **3m** and **3n** to the growth of Detroit 551 are more than 3 μM, suggesting that these compounds are less toxic to normal human skin fibroblasts compared to HCT116 colorectal cancer cells (Table 2).

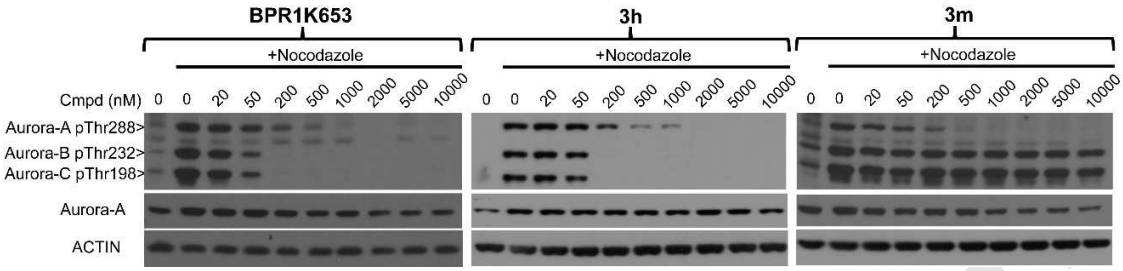

Fig. 2. Representative cellular inhibition profile of the compounds to Aurora kinases. Immunoblot of phosphorylated Aurora-A (Thr288), Aurora-B (Thr232) and Aurora-C (Thr198). HCT116 cells were arrested in the M phase with 24 h treatment of 200 nM nocodazole, followed by 1 h treatment with the indicated compounds at various concentrations. ACTIN immunoblot was included as a loading control.

Table 2. Biological evaluation of the prepared compounds.

Compd.	R1	R2	R3	pAURKA IC_{50}[a] (nM)	pAURKB IC_{50}[a] (nM)	Cellular IC_{50} Ratio A/B	HCT116 viability IC_{50}[b] (nM)	Detroit 551 viability IC_{50}[b] (μM)
BPR1K653		H	H	73.4	23.7	3.1/1	70	3.1
3a	H	H	H	389.6	191.2	2/1	153	7.3
3h	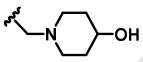	H	H	1513.0	132.6	11.4/1	310	3.5
3m	H		H	59.9	>10,000	1/(>166.9)	578	5.0
3n	H		H	132.2	>10,000	1/(>75.6)	342	9.7

[a] IC_{50} values are calculated from Western blot profiles (Fig. 2) of 9 titration points.
[b] IC_{50} values are calculated from a duplicated, 10-point titration.

2.2.3 Effect of the synthesized compounds on mitotic progression

Phosphorylation on the serine 10 of histone H3 (pHH3Ser10) is widely used as an immunomarker specific to cells undergoing mitosis [38]. To determine the effect of the newly synthesized compounds on mitotic progression, we measured pHH3Ser10-positive (i.e. mitotic index, MI) HeLa cells released from thymidine block at various time points (Fig. 3A). We used HeLa instead of HCT116 in mitotic progression analysis due to the high synchronization efficiency of this cell line by thymidine block [39]. Compared to mock and DMSO-treated controls, treatment with compound **3m** significantly increased MI at 10-12 hours post thymidine block (Fig. 3B-C), suggesting compound **3m** can delay mitotic progression – an effect which should be attributed to Aurora-A kinase inhibition. In contrast, **BPR1K653** and compound **3h** drastically reduced MI (Fig. 3B-C), suggesting that these two compounds are more potent Aurora-B kinase inhibitors. Compound **3a**, which does not possess isoform-inhibition selectivity, slightly increased, MI at 10-12 hours post thymidine block, but to a lesser degree compared to compound **3m**. These data indicate that the cellular phenotype of the compounds on mitotic progression correlated with their inhibition selectivity to Aurora-A or Aurora-B.

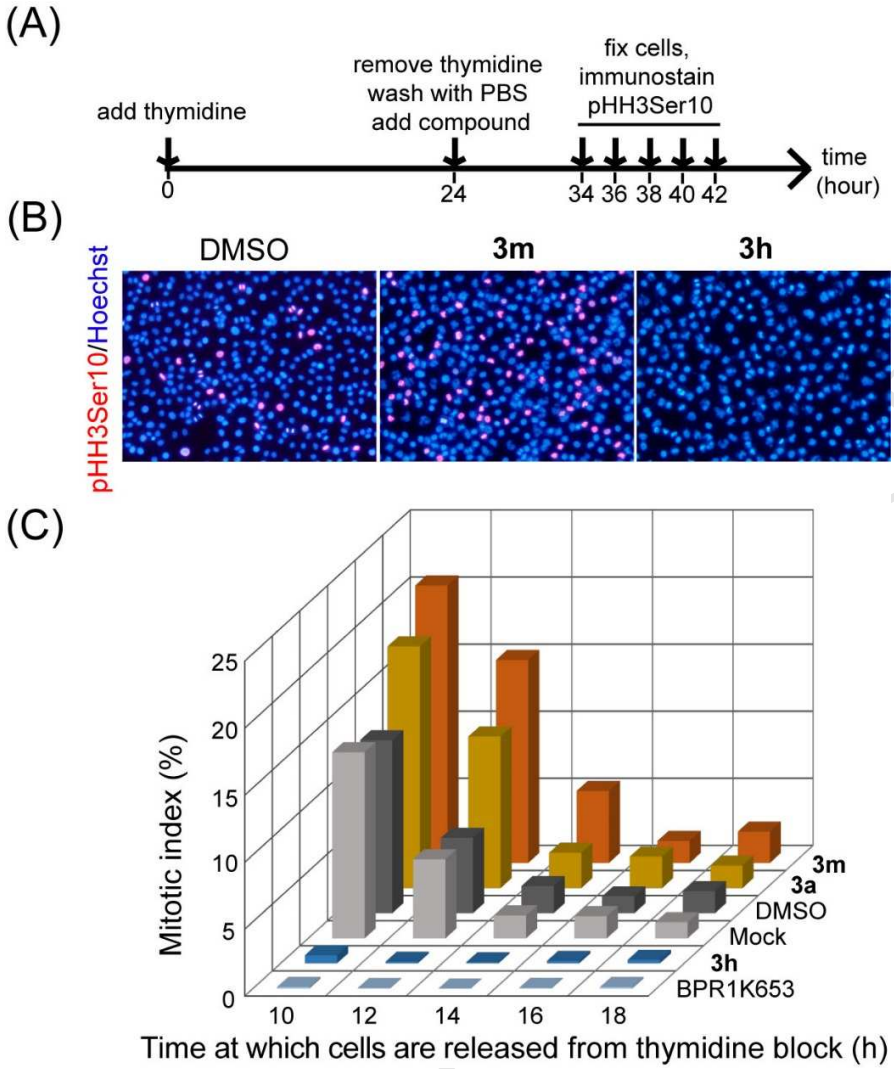

Fig. 3. (A) Schematic illustration of the protocol for the functional study of the compounds on mitotic progression. (B) Immunofluorescence staining of pHH3Ser10 (red) on compound-treated cells fixed at 12 hours after release from thymidine block. Nuclei were counterstained with Hoechst 33342 (blue). Representative images were shown. Percentage of pHH3Ser10-positive cells were quantified in (C) as shown as mitotic index (MI). About 2000-3000 cells were quantified using MetaMorph software in each experimental condition.

2.3. Molecular docking study

2.3.1. Structure alignment of Aurora-A and Aurora-B

A typical ATP binding pocket of a kinase can be divided into six sub-pockets: the adenine pocket, ribose pocket, phosphate pocket, hydrophobic pocket-I, hydrophobic pocket-II and back pocket [40, 41]. The protein sequences in the ATP-binding site of Aurora-A and Aurora-B are highly conserved. Only three amino acids are not aligned: Leu215, Thr217, and Arg220 in Aurora-A; and Arg159, Glu161, and Lys164 in Aurora-B (Fig. S1, supplementary data) [42]. The interaction between imidazo[4,5-*b*]pyridine-derived small molecules with the Thr217 residue of Aurora-A has been reported to play a critical role in governing the isoform selectivity for Aurora-A inhibition [43]. How the other sub-pockets contribute to the inhibition selectivity of Aurora isoforms is not clear.

Our previous structural analysis suggested that the phenylurea derivative on the 4-position of furanopyrimidine extended to the back pocket of Aurora-A [29, 44]. To understand the structural differences in the back pocket of Aurora isoforms, we compared X-ray profiles of human Aurora-A (PDB ID: 2W1C, in complex with an Aurora inhibitor) and Aurora-B (PDB ID: 4AF3, in complex with INCENP and VX-680) (Fig. 4) [10, 45]. The protein sequences of Aurora-A and Aurora-B in the region of back pocket are very

well aligned (Fig. 4A). However, a surface modeling analysis determined that the spatial vacancy in the back pocket is about 70% greater in Aurora-B than in Aurora-A (179.59 $Å^3$ in Aurora-A; 310.33 $Å^3$ in Aurora-B, Fig. 4B). In addition, residues Gln177, Glu181, Gln185 in the αC-helix of Aurora-A and the corresponding Gln121, Glu125, Gln129 in Aurora-B showed more significant deviation than residues in the β3-β4-β5 three-stranded antiparallel beta sheet (Fig. 4C).

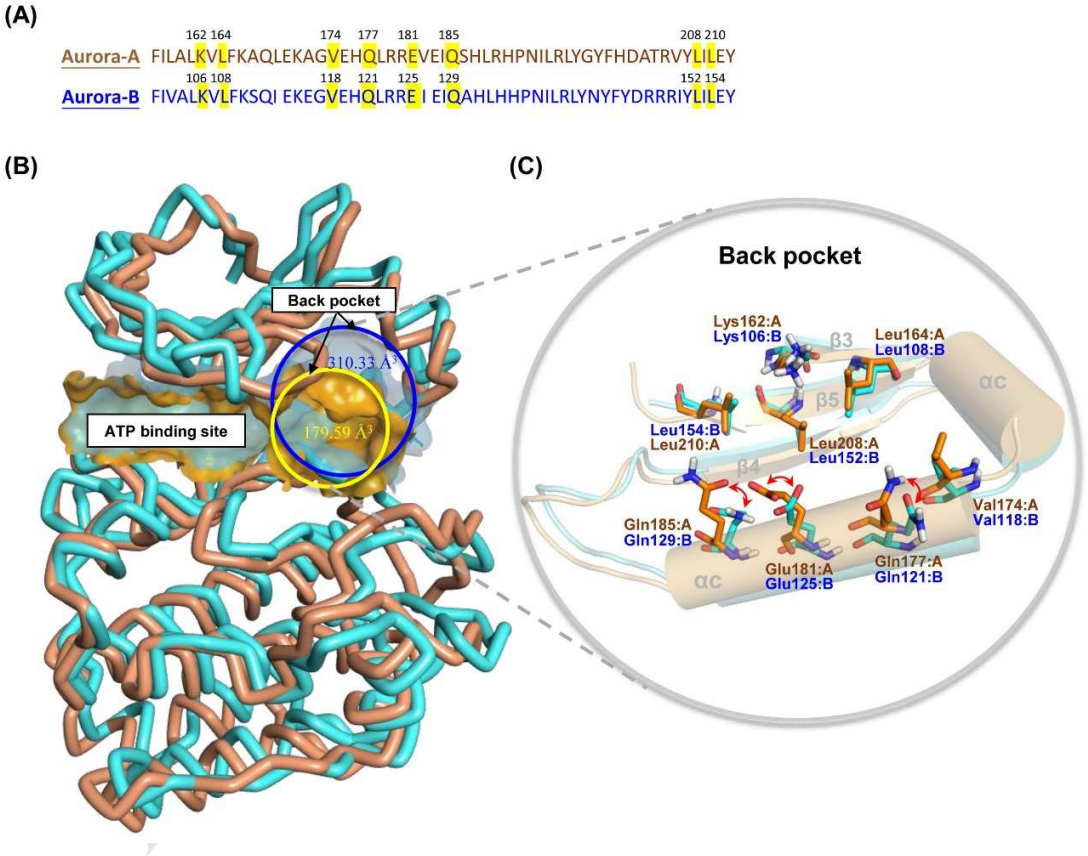

Fig. 4. (A) Alignment of partial amino acid sequence of Aurora-A and Aurora-B. Residues that contribute to the back pocket are highlighted in yellow background. (B) Structure alignment of Aurora-A (PDB ID: 2W1C, khaki) and Aurora-B (PDB ID: 4AF3, cyan). Surface modeling of ATP-binding site and back pocket are presented in the same color. (C) Conformation variation in the back pocket of Aurora-A (khaki) and Aurora-B

(blue).

2.3.2. Molecular docking for selective inhibitors

The biological evaluation results indicated that compound **3a** (which does not contain substitution on the phenylurea) showed near equal inhibition to Aurora-A and Aurora-B, and the addition of substituents on the ortho or meta position of the phenylurea resulted in increased selectivity for Aurora-B or Aurora-A, respectively (Table 1). The molecular docking analysis of compound **3a** in complex with Aurora-A and Aurora-B suggested that the ortho position of the phenyl group of **3a** presented more space in complex with Aurora-B than in Aurora-A, while the meta-position of the phenyl group was more distant from Aurora-A than Aurora-B (Fig. 5). Therefore, extending moieties at the ortho or meta positions of the phenylurea in **3a** may affect the inhibition selectivity for Aurora-A or Aurora-B.

The molecular docking structure of Aurora-A in complex with compound **3n** suggested that the ethyl amino group not only has a strong CH-π hydrophobic interaction with Phe144 of Aurora-A, but also forms an intramolecular CH-π interaction with its phenyl group (Fig. 6A). This intramolecular hydrophobic interaction enables better fitting of compound **3n** in the back pocket of Aurora-A. On the other hand, functional groups such as the piperidinyl and 4-hydroxypiperidinyl groups in compounds **3p** and **3q** may be

too large to be accommodated in the back pocket of Aurora-A, thereby decreasing the potency with which they inhibit Aurora-A (Table 1). In contrast, compound **3h** (which bear a 4-hydroxypiperidinyl derivative on the ortho position of the phenylurea)**,** presented about 3-fold better enzymatic activity to Aurora-B than Aurora-A (Table, 1). A molecular docking analysis of compound **3h** with Aurora-A and Aurora-B suggested that the -OH at the 4-position of the piperidine in **3h** may form hydrogen bonding with residue Gln121 in Aurora-B (Fig. 6B), while causing a steric obstacle with Gln177 of Aurora-A. Conversely, compounds **3f** and **3g** (which fail to form hydrogen bonding with Gln121 of Aurora-B) did not show an inhibition preference to either Aurora-A or Aurora-B (Table 1).

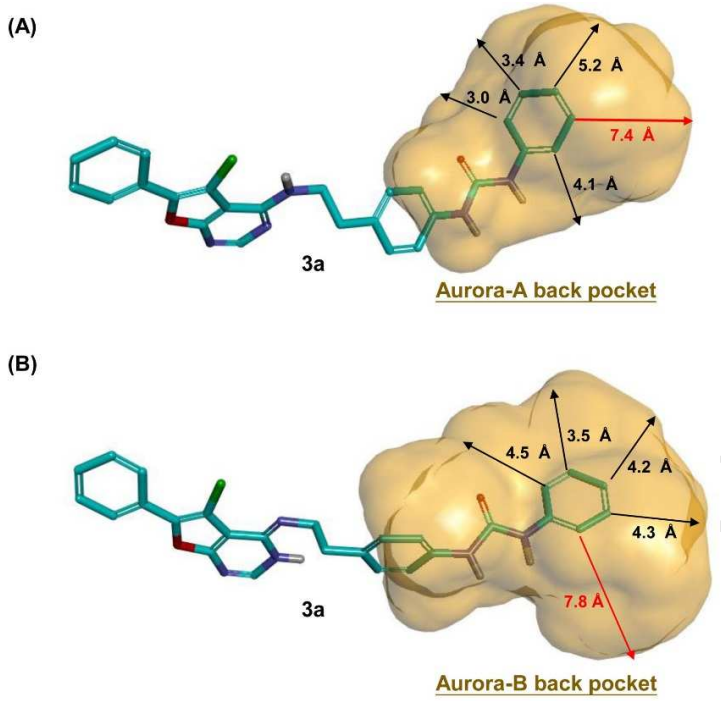

Fig. 5. (A) The docking analysis for compound **3a** with Aurora-A. The back pocket of Aurora-A is displayed in transparent surface. (B) The docking analysis for compound **3a** with Aurora-B. The back pocket of Aurora-B is displayed in transparent surface. Approximate distance of the molecules at the indicated positions are shown.

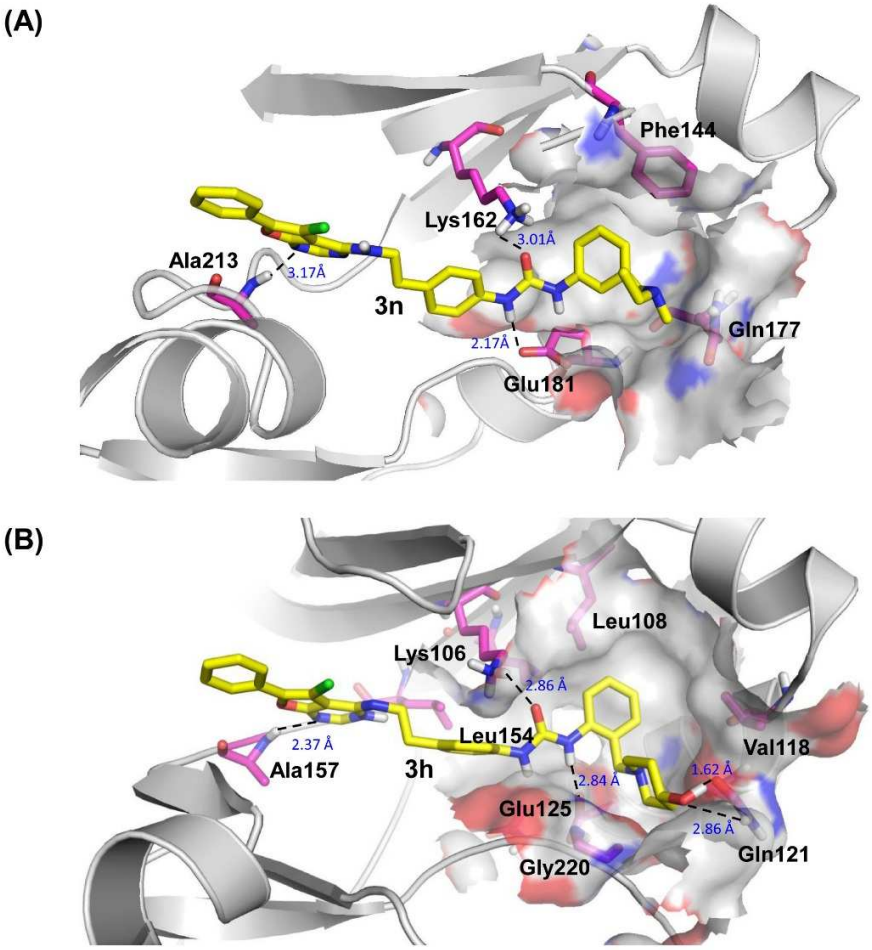

Fig. 6. (A) The docking analysis for compound **3n** (yellow) with Aurora-A. Compound **3n** forms hydrogen bonding with Lys162, Glu181, and Ala213. Compound **3n** has a strong hydrophobic effect with Phe144. (B) The docking analysis for compound **3h** (yellow) with Aurora-B. Compound **3h** forms hydrogen bonding with Lys106, Gln121, Glu125, and Ala157.

3. Conclusions

The molecular and cellular functions of Aurora kinases -A, -B and -C are distinct in space and time. Therefore, small molecules that selectively inhibit Aurora isoforms are expected to show different mechanisms of action, and thus potentially target different subsets of patients in clinical applications. In this study, we discovered **BPR1K653** (1-(4-(2-((5-chloro-6-phenylfuro[2,3-d]pyrimidin-4-yl)amino)ethyl)phenyl)-3-phenyl)ure a) derivatives **3m** and **3n** bearing substituents at the meta position of the phenylurea, and found that they displayed a high degree of inhibition selectivity for Aurora-A over Aurora-B in both enzymatic and cellular assays, while the superior Aurora-B inhibition selectivity was maintained in an ortho derivative **3h**. The molecular docking analysis of the compounds with Aurora-A and Aurora-B suggested that the spatial variation in the back pocket can be used as a design principle for isoform-specific inhibitors. This selectivity design strategy is different from previous compounds which target the non-conserved amino acids in the ATP-binding site of Aurora-A and Aurora-B. The pharmacokinetic and pharmacodynamic properties of the lead compounds with the best Aurora-A selectivity are currently being evaluated for *in vivo* animal multi-drug resistant tumor xenograft models.

4. Experimental

4.1. Chemistry

Commercially available reagents were used as supplied, unless otherwise stated. Reactions requiring anhydrous conditions were performed in flame-dried glassware, and cooled under an argon or nitrogen atmosphere. All reactions were carried out under positive pressure of argon or nitrogen, and monitored by analytical thin layer chromatography using glass-backed plates (5 × 10 cm) pre-coated with silica gel 60 F_{254}, as supplied by Merck; zones were detected visually under UV irradiation (254 nm) or by spraying with phosphomolybdic acid reagent (Sigma-Aldrich, USA) followed by heating to 80 ℃. Flash column chromatography was used routinely for purification and separation of product mixtures using silica gel 60 of 230−400 mesh size as supplied by Merck. ^{1}H and ^{13}C NMR spectra were recorded on Varian Mercury-300 or Varian Mercury-400 (Fig. S3 supplementary data). Chloroform-*d* or dimethyl sulfoxide-d_6 was used as the solvent and TMS (δ 0.00 ppm) as an internal standard. Chemical shift values are reported in ppm relative to the TMS in delta (δ) units. Multiplicities are recorded as s (singlet), brs (broad singlet), d (doublet), t (triplet), q (quartet), quint (quintet), sep (septet), dd (doublet of doublets), dt (doublet of triplets), and m (multiplet). Coupling constants (*J*) are expressed in hertz. Electrospray mass spectra (ESMS) were recorded as

m/z values using an Agilent 1100 MSD mass spectrometer. High-resolution mass spectra were recorded under ESI-TOF mass spectroscopy conditions. All test compounds displayed more than 95% purity as determined by a Hitachi 2000 series HPLC system using a C-18 column (Agilent Eclipse XDB-C18 5 μm, 4.6 mm × 150 mm, USA). Mobile phase A: acetonitrile; mobile phase B: 2 mM ammonium acetate aqueous solution containing 0.1% formic acid. The gradient system started from A:B (10% : 90%) to A:B (90% : 10%) with a flow rate of 0.5 mL/min and the injection volume was 20 μL. The system was operated at 25 °C. Peaks were detected at 254 nm. IUPAC nomenclature of compounds was determined with ACD/Name Pro software.

*4.2. N-(4-aminophenethyl)-5-chloro-6-phenylfuro[2,3-d]pyrimidin-4-amine (**2**)*

Compound (**1**) [30] (1 g, 3.77 mmol) and 4-(2-aminoethyl)aniline (512 mg, 3.77 mmol) in EtOH (20 mL) were heated to reflux for 1 h. The reaction mixture was poured into water, the precipitate was filtered and washed with water several times to afford **2** (1.18 g, 86%); ^{1}H NMR (400 MHz, $CDCl_3$) δ 8.29 (s, 1H), 8.00 (d, J = 7.2 Hz, 2H), 7.51 (t, J = 7.2 Hz, 2H), 7.44 (t, J = 7.2 Hz, 1H), 7.05 (d, J = 8.4 Hz, 2H), 6.71 (d, J = 8.4 Hz, 2H), 3.79 (t, J = 7.0 Hz, 2H), 2.88 (t, J = 7.0 Hz, 2H); LCMS (ESI) *m/z*: 365.2 $[M+H]^+$.

*4.3. General procedure for the synthesis of compounds **3a, 3c, 3d, 3i, 3r-3t***

The general procedure is illustrated below with compound **3a** as a specific example.

1-(4-(2-((5-chloro-6-phenylfuro[2,3-d]pyrimidin-4-yl)amino)ethyl)phenyl)-3-Phenyl)urea

(3a)

A mixture of compound **2** (100 mg, 0.27 mmol) and phenyl isocyanate (0.059 ml, 0.54 mmol) in CH_2Cl_2 (2 mL) was stirred under an argon atmosphere at room temperature. After 4 h, the reaction mixture was concentrated *in vacuo*. The residue was purified by silica gel column chromatography with MeOH/DCM (2:98) to give the title compound **3a** (86 mg, 66%); ^{1}H NMR (400 MHz, DMSO-*d6*) δ 8.63 (dd, *J* = 9.6, 3.6 Hz, 2H), 8.37 (s, 1H), 7.98 (d, *J* = 8.3 Hz, 2H), 7.57 (t, *J* = 8.3 Hz, 2H), 7.48 (t, *J* = 8.3 Hz, 1H), 7.44 (d, *J* = 8.4 Hz, 2H), 7.39 (d, *J* = 8.0 Hz, 2H), 7.29-7.25 (m, 3H), 7.19 (d, *J* = 8.4 Hz, 2H), 6.97 (t, *J* = 8.0 Hz, 1H), 3.73 (q, *J* = 7.6 Hz, 2H), 2.87 (t, *J* = 7.6 Hz, 2H); ^{13}C NMR (100 MHz, DMSO-*d6*) δ 163.46, 156.45, 154.91, 152.54, 144.08, 139.75, 137.89, 132.56, 129.35, 129.12, 139.00, 128.76, 127.61, 125.66, 121.74, 118.39, 118.14, 104.47, 100.56, 42.23, 34.20; LCMS (ESI) *m/z*: 484.2 $[M+H]^+$; HRMS (ESI) calcd for $C_{27}H_{22}ClN_5O_2$ $[M+H]^+$ m/z 484.1540; found: 484.1546; HPLC purity = 99.7%, *t*R = 42.99 min.

*4.4. General procedure for the synthesis of compounds **3b, 3e-3h, 3j-3q, 3u-3y***

The general procedure is illustrated below with compound **3b** as a specific example.

*1-(4-(2-((5-chloro-6-phenylfuro[2,3-d]pyrimidin-4-yl)amino)ethyl)phenyl)-3-(o-tolyl) urea (**3b**)*

To a solution of compound **2** (100 mg, 0.27 mmol) in 1,4-dioxane (2.0 mL) at room temperature were added phenyl *o*-tolylcarbamate (246 mg, 1.08 mmol) and triethylamine (0.38 ml, 2.7 mmol). The mixture was stirred under argon atmosphere for 10 h at 120 ^{o}C. After the reaction was completed, the reaction mixture was poured into water and extracted with ethyl acetate. The organic layer was washed with brine, dried over anhydrous Na_2SO_4, and concentrated *in vacuo*. The residue was purified by silica gel column chromatography with MeOH/DCM (2:98) to give the title compound **3b** (47 mg, 35%); ^{1}H NMR (400 MHz, DMSO-*d6*) δ 8.97 (s, 1H), 8.38 (s, 1H), 7.99 (d, *J* = 7.2 Hz, 2H), 7.88 (s, 1H), 7.84 (d, *J* = 7.7 Hz, 1H), 7.57 (t, *J* = 7.2 Hz, 2H), 7.49 (t, *J* = 7.2 Hz, 1H), 7.40 (d, *J* = 8.4 Hz, 2H), 7.28 (brs, 1H), 7.20-7.18 (m , 3H), 7.13 (t, *J* = 7.7 Hz, 1H), 6.93 (t, *J* = 7.7 Hz, 1H), 3.75 (q, *J* = 7.3 Hz, 2H), 2.89 (t, *J* = 7.3 Hz, 2H), 2.30 (s, 3H); ^{13}C NMR (100 MHz, DMSO-*d6*) δ 163.44, 156.43, 154.90, 152.66, 144.05, 138.08, 137.47, 132.43, 130.17, 129.33, 129.10, 129.06, 127.62, 127.36, 126.14, 125.63, 122.56, 120.91, 118.21, 104.47, 100.56, 42.25, 34.20, 17.90; LCMS (ESI) *m/z*: 498.2 $[M+H]^+$; HRMS (ESI) calcd for $C_{28}H_{24}ClN_5O_2$ $[M+H]^+$ m/z 498.1697; found: 498.1711; HPLC purity = 96.8%, *t*R = 43.71 min.

*4.4.1. 1-(4-(2-((5-chloro-6-phenylfuro[2,3-d]pyrimidin-4-yl)amino)ethyl)phenyl)-3-(2-ethylphenyl)urea (**3c**)*

Following the similar reaction and workup procedures for **3a**, the residue was purified by silica gel column chromatography with MeOH/DCM (2:98) to give **3c**. Yield: 47%; ^{1}H NMR (400 MHz, DMSO-*d6*) δ 8.98 (s, 1H), 8.38 (s, 1H), 7.99 (d, *J* = 7.2 Hz, 2H), 7.87 (s, 1H), 7.80 (d, *J* = 7.6 Hz, 1H), 7.57 (t, *J* = 7.2 Hz, 2H), 7.49 (t, *J* = 7.2 Hz, 1H), 7.41 (d, *J* = 8.4 Hz, 2H), 7.28 (brs, 1H), 7.20-7.17 (m, 3H), 7.14 (t, *J* = 7.6 Hz, 1H), 6.99 (t, *J* = 7.6 Hz, 1H), 3.75 (q, *J* = 7.4 Hz, 2H), 2.89 (t, *J* = 7.4 Hz, 2H), 2.60 (q, *J* = 7.6 Hz, 2H), 1.17 (t, *J* = 7.6 Hz, 3H); ^{13}C NMR (100 MHz, DMSO-*d6*) δ 163.45, 156.43, 154.91, 152.87, 144.05, 138.11, 136.59, 133.61, 132.40, 129.34, 129.12, 129.06, 128.39, 127.62, 126.04, 125.64, 123.07, 121.94, 118.18, 104.47, 100.56, 42.26, 34.20, 23.80, 14.29; LCMS (ESI) *m/z*: 512.3 $[M+H]^+$; HRMS (ESI) calcd for $C_{29}H_{26}ClN_5O_2$ $[M+Na]^+$ m/z 534.1673; found: 534.1682; HPLC purity = 99.5%, *t*R = 45.37 min.

*4.4.2. 1-(4-(2-((5-chloro-6-phenylfuro[2,3-d]pyrimidin-4-yl)amino)ethyl)phenyl)-3-(2-isopropylphenyl)urea (**3d**)*

Following the similar reaction and workup procedures for **3a**, the residue was purified by silica gel column chromatography with MeOH/DCM (2:98) to give **3d**. Yield: 34%; ^{1}H NMR (400 MHz, DMSO-*d6*) δ 8.90 (s, 1H), 8.38 (s, 1H), 7.99 (d, *J* = 8.0 Hz, 2H), 7.90 (s, 1H), 7.66 (d, *J* = 7.6 Hz, 1H), 7.57 (t, *J* = 8.0 Hz, 2H), 7.49 (t, *J* = 8.0 Hz, 1H), 7.40 (d, *J* = 8.0 Hz, 2H), 7.28-7.26 (m, 2H), 7.19 (d, *J* = 8.0 Hz, 2H), 7.14 (t, *J* = 7.6

Hz, 1H), 7.06 (t, *J* = 7.6 Hz, 1H), 3.75 (q, *J* = 7.6 Hz, 2H), 3.14 (sep, *J* = 6.8 Hz, 1H), 2.89 (t, *J* = 7.6 Hz, 2H), 1.19 (t, *J* = 6.8 Hz, 6H); ^{13}C NMR (100 MHz, DMSO-*d6*) δ 163.44, 156.42, 154.88, 153.14, 144.04, 139.28, 138.19, 135.56, 132.33, 129.30, 129.08, 129.03, 127.61, 125.70, 125.61, 125.21, 123.80, 123.44, 118.16, 104.47, 100.56, 42.25, 34.20, 26.79, 23.12; LCMS (ESI) *m/z*: 526.3 $[M+H]^+$; HRMS (ESI) calcd for $C_{30}H_{28}ClN_5O_2$ $[M+H]^+$ m/z 526.2010; found: 526.2025; HPLC purity = 97.7%, *t*R = 46.35 min.

*4.4.3. 1-(4-(2-((5-chloro-6-phenylfuro[2,3-d]pyrimidin-4-yl)amino)ethyl)phenyl)-3-(2-isobutylphenyl)urea (**3e**)*

Following the similar reaction and workup procedures for **3b**, the residue was purified by silica gel column chromatography with MeOH/DCM (2:98) to give **3e**. Yield: 34%; ^{1}H NMR (400 MHz, DMSO-*d6*) δ 8.95 (s, 1H), 8.37 (s, 1H), 7.98 (d, *J* = 7.4 Hz, 2H), 7.78 (s, 1H), 7.74 (d, *J* = 7.4 Hz, 1H), 7.57 (t, *J* = 7.4 Hz, 2H), 7.48 (t, *J* = 7.4 Hz, 1H), 7.41 (d, *J* = 7.6 Hz, 2H), 7.25 (brs, 1H), 7.19 (d, *J* = 7.6 Hz, 2H), 7.16-7.11 (m, 2H), 6.98 (t, *J* = 7.4 Hz, 1H), 3.75 (q, *J* = 7.2 Hz, 2H), 2.89 (t, *J* = 7.2 Hz, 2H), 2.47 (d, *J* = 6.8 Hz, 2H), 1.88-1.81 (m, 1H), 0.88 (d, *J* = 6.8 Hz, 6H); ^{13}C NMR (100 MHz, DMSO-*d6*) δ 163.45, 156.43, 154.91, 152.91, 144.06, 138.14, 136.86, 132.38, 131.55, 130.30, 129.33, 129.10, 129.03, 127.61, 126.09, 125.64, 122.88, 122.73, 118.23, 104.47, 100.56, 42.25,

39.72, 34.20, 28.22, 22.25; LCMS (ESI) *m/z*: 540.3 $[M+H]^+$; HRMS (ESI) calcd for $C_{31}H_{30}ClN_5O_2$ $[M+H]^+$ m/z 540.2166; found: 540.2161; HPLC purity = 98.5%, *t*R = 48.37 min.

*4.4.4. 1-(4-(2-((5-chloro-6-phenylfuro[2,3-d]pyrimidin-4-yl)amino)ethyl)phenyl)-3-(3-((diethylamino)methyl)phenyl)urea (**3f**)*

Following the similar reaction and workup procedures for **3b**, the residue was purified by silica gel column chromatography with MeOH/DCM (5:95) to give **3f**. Yield: 62%; ^{1}H NMR (400 MHz, DMSO-*d6*) δ 9.35 (s, 1H), 9.08 (s, 1H), 8.37 (s, 1H), 7.97 (d, *J* = 7.4 Hz, 2H), 7.76 (d, *J* = 7.8 Hz, 1H), 7.56 (t, *J* = 7.4 Hz, 2H), 7.48 (t, *J* = 7.4 Hz, 1H), 7.40 (d, *J* = 8.0 Hz, 2H), 7.26-7.18 (m, 5H), 6.94 (t, *J* = 7.8 Hz, 1H), 3.75 (q, *J* = 6.2 Hz, 2H), 3.53 (s, 2H), 2.89 (t, *J* = 6.2 Hz, 2H), 2.44 (q, *J* = 6.8 Hz, 4H), 0.96 (t, *J* = 6.8 Hz, 6H); ^{13}C NMR (75 MHz, DMSO-*d6*) δ 163.49, 156.48, 154.96, 152.82, 144.12, 138.97, 138.15, 132.80, 129.63, 129.42, 129.17, 128.96, 127.72, 127.64, 127.28, 125.69, 122.10, 121.54, 119.52, 104.52, 100.61, 55.30, 45.88, 42.27, 34.24, 10.73; LCMS (ESI) *m/z*: 569.3 $[M+H]^+$; HRMS (ESI) calcd for $C_{32}H_{33}ClN_6O_2$ $[M+H]^+$ m/z 569.2432; found: 569.2436; HPLC purity = 96.6%, *t*R = 29.25 min.

*4.4.5. 1-(4-(2-((5-chloro-6-phenylfuro[2,3-d]pyrimidin-4-yl)amino)ethyl)phenyl)-3-(2-(piperidin-1-ylmethyl)phenyl)urea (**3g**)*

Following the similar reaction and workup procedures for **3b**, the residue was purified by silica gel column chromatography with MeOH/DCM (5:95) to give **3g**. Yield: 20%; ^{1}H NMR (300 MHz, DMSO-*d6*) δ 9.10 (s, 1H), 9.06 (s, 1H), 8.38 (s, 1H), 7.99 (d, *J* = 7.3 Hz, 2H), 7.93 (d, *J* = 7.6 Hz, 1H), 7.58 (t, *J* = 7.3 Hz, 2H), 7.49 (t, *J* = 7.3 Hz, 1H), 7.40 (d, *J* = 8.4 Hz, 2H), 7.28 (brs, 1H), 7.22-7.19 (m, 3H), 7.16 (d, 7.6 Hz, 1H), 6.93 (t, *J* = 7.6 Hz, 1H), 3.76 (q, *J* = 7.2 Hz, 2H), 3.46 (s, 2H), 2.90 (t, *J* = 7.2 Hz, 2H), 2.38-2.24 (m, 4H), 1.57-1.44 (m, 4H), 1.44-1.34 (m, 2H); ^{13}C NMR (100 MHz, DMSO-*d6*) δ 163.47, 156.44, 154.91, 152.85, 144.08, 138.89, 138.05, 132.82, 129.86, 129.35, 129.13, 120.98, 127.62, 127.46, 126.27, 125.66, 121.84, 120.67, 119.45, 104.47, 100.56, 60.97, 53.58, 42.22, 34.22, 25.22, 23.88; LCMS (ESI) *m/z*: 581.3 $[M+H]^+$; HRMS (ESI) calcd for $C_{33}H_{33}ClN_6O_2$ $[M+H]^+$ m/z 581.2432; found: 581.2428; HPLC purity = 99.2%, *t*R = 29.55 min.

*4.4.6. 1-(4-(2-((5-chloro-6-phenylfuro[2,3-d]pyrimidin-4-yl)amino)ethyl)phenyl)-3-(2-((4-hydroxypiperidin-1-yl)methyl)phenyl)urea (**3h**)*

Following the similar reaction and workup procedures for **3b**, the residue was purified by silica gel column chromatography with MeOH/DCM (10:90) to give **3h**. Yield: 30%; ^{1}H NMR (300 MHz, $CDCl_3$) δ 8.40 (s, 1H), 8.03 (d, *J* = 7.5 Hz, 2H), 7.98 (d, *J* = 7.4 Hz, 1H), 7.48 (t, *J* = 7.5 Hz, 2H), 7.40 (t, *J* = 7.5 Hz, 1H), 7.37 (d, *J* = 8.2 Hz, 2H),

7.32 (d, *J* = 7.4 Hz, 1H), 7.26 (d, *J* = 8.2 Hz, 2H), 7.20 (brs, 1H), 7.07 (d, *J* = 7.4 Hz, 1H), 6.98 (t, *J* = 7.4 Hz, 1H), 6.46 (brs, 1H), 5.94 (brs, 1H), 3.90 (q, *J* = 6.4 Hz, 2H), 3.55-3.53 (m, 1H), 3.53 (s, 2H), 2.99 (t, *J* = 6.4 Hz, 2H), 2.54-2.52 (m, 2H), 2.03-2.01 (m, 2H), 1.42-1.35 (m, 2H), 0.88-0.83 (m, 2H); ^{13}C NMR (100 MHz, DMSO-*d6*) δ 163.45, 156.44, 154.91, 152.97, 144.07, 138.89, 138.07, 132.82, 130.24, 129.34, 129.12, 129.01×2, 127.63×2, 125.64, 122.17, 121.16, 119.32, 104.50, 100.59, 65.73, 59.81, 50.34, 42.25, 34.25, 33.64; LCMS (ESI) *m/z*: 597.3 $[M+H]^+$; HRMS (ESI) calcd for $C_{33}H_{33}ClN_6O_3$ $[M+H]^+$ m/z 597.2381; found: 597.2379; HPLC purity = 99.0%, *t*R = 27.22 min.

*4.4.7. 1-(4-(2-((5-chloro-6-phenylfuro[2,3-d]pyrimidin-4-yl)amino)ethyl)phenyl)-3-(m-tolyl)urea (**3i**)*

Following the similar reaction and workup procedures for **3a**, the residue was purified by silica gel column chromatography with MeOH/DCM (2:98) to give **3i**. Yield: 39%; ^{1}H NMR (400 MHz, DMSO-*d6*) δ 8.69 (brs, 1H), 8.65 (brs, 1H), 8.38 (s, 1H), 7.99 (d, *J* = 7.7 Hz, 2H), 7.57 (t, *J* = 7.7 Hz, 2H), 7.49 (t, *J* = 7.7 Hz, 1H), 7.40 (d, *J* = 8.0 Hz, 2H), 7.29 (s, 1H), 7.27 (brs, 1H), 7.22 (d, *J* = 7.7 Hz, 1H), 7.18 (d, *J* = 8.0 Hz, 2H), 7.14 (t, *J* = 7.7 Hz, 1H), 6.77 (d, *J* = 7.7 Hz, 1H), 3.75 (q, *J* = 7.6 Hz, 2H), 2.89 (t, *J* = 7.6 Hz, 2H), 2.27 (s, 3H); ^{13}C NMR (100 MHz, DMSO-*d6*) δ 163.44, 156.43, 154.90, 152.53, 144.05, 139.67, 137.93×2, 132.52, 129.32, 129.10, 129.01, 128.61, 127.62, 125.63,

122.49, 118.65, 118.34, 115.32, 104.47, 100.56, 42.24, 34.20, 21.24; LCMS (ESI) *m/z*: 498.2 $[M+H]^+$; HRMS (ESI) calcd for $C_{28}H_{24}ClN_5O_2$ $[M+H]^+$ m/z 498.1697; found: 498.1686; HPLC purity = 96.1%, *t*R = 44.29 min.

*4.4.8. 1-(4-(2-((5-chloro-6-phenylfuro[2,3-d]pyrimidin-4-yl)amino)ethyl)phenyl)-3-(3-ethylphenyl)urea (**3j**)*

Following the similar reaction and workup procedures for **3b**, the residue was purified by silica gel column chromatography with MeOH/DCM (2:98) to give **3j**. Yield: 64%; ^{1}H NMR (400 MHz, DMSO-*d6*) δ 8.77 (brs, 1H), 8.76 (brs, 1H), 8.38 (s, 1H), 7.99 (d, *J* = 7.5 Hz, 2H), 7.57 (t, *J* = 7.5 Hz, 2H), 7.49 (t, *J* = 7.5 Hz, 1H), 7.40 (d, *J* = 8.6 Hz, 2H), 7.32 (s, 1H), 7.27 (brs, 1H), 7.24 (d, *J* = 7.9 Hz, 1H), 7.18 (d, *J* = 8.6 Hz, 2H), 7.16 (t, *J* = 7.9 Hz, 1H), 6.80 (d, *J* = 7.9 Hz, 1H), 3.75 (q, *J* = 8.0 Hz, 2H), 2.89 (t, *J* = 8.0 Hz, 2H), 2.56 (q, *J* = 7.6 Hz, 2H), 1.17 (t, *J* = 7.6 Hz, 3H); ^{13}C NMR (100 MHz, DMSO-*d6*) δ 163.44, 156.42, 154.89, 152.55, 144.33, 144.04, 139.73, 137.94, 132.52, 129.31, 129.09, 129.01, 128.67, 127.62, 125.62, 121.29, 118.35, 117.51, 115.60, 104.47, 100.56, 42.25, 34.21, 28.31, 15.58; LCMS (ESI) *m/z*: 512.3 $[M+H]^+$; HRMS (ESI) calcd for $C_{29}H_{26}ClN_5O_2$ $[M+H]^+$ m/z 512.1853; found: 512.1868; HPLC purity = 97.5%, *t*R = 46.54 min.

4.4.9. 1-(4-(2-((5-chloro-6-phenylfuro[2,3-d]pyrimidin-4-yl)amino)ethyl)phenyl)-3-(3-

*isopropylphenyl)urea (**3k**)*

Following the similar reaction and workup procedures for **3b**, the residue was purified by silica gel column chromatography with MeOH/DCM (2:98) to give **3k**. Yield: 45%; ^{1}H NMR (400 MHz, $CDCl_3$) δ 8.41 (s, 1H), 8.01 (d, J = 7.2 Hz, 2H), 7.47 (t, J = 7.2 Hz, 2H), 7.40 (t, J = 7.2 Hz, 1H), 7.34 (d, J = 8.4 Hz, 2H), 7.30 (t, J = 8.0 Hz, 1H), 7.24 (d, J = 8.4 Hz, 2H), 7.22 (s, 1H), 7.15 (d, J = 8.0 Hz, 1H), 7.03 (d, J = 8.0 Hz, 1H), 6.56 (brs, 1H), 6.47 (brs, 1H), 5.89 (brs, 1H), 3.89 (q, J = 6.8 Hz, 2H), 2.98 (t, J = 6.8 Hz, 2H), 2.89 (sep, J = 6.8 Hz, 1H), 1.24 (d, J = 6.8 Hz, 6H); ^{13}C NMR (100 MHz, DMSO-*d6*) δ 163.46, 156.44, 154.91, 152.56, 149.01, 144.07, 139.70, 137.92, 132.52, 129.35, 129.12, 129.0, 128.66, 127.62, 125.65, 119.84, 118.37, 116.12, 115.77, 104.47, 100.56, 42.25, 34.89, 33.50, 23.88; LCMS (ESI) *m/z*: 526.3 $[M+H]^+$; HRMS (ESI) calcd for $C_{30}H_{28}ClN_5O_2$ $[M+H]^+$ m/z 526.2010; found: 526.2025; HPLC purity = 99.7%, *t*R = 47.87 min.

*4.4.10. 1-(4-(2-((5-chloro-6-phenylfuro[2,3-d]pyrimidin-4-yl)amino)ethyl)phenyl)-3-(3-isobutylphenyl)urea (**3l**)*

Following the similar reaction and workup procedures for **3b**, the residue was purified by silica gel column chromatography with MeOH/DCM (2:98) to give **3l**. Yield: 57%; ^{1}H NMR (400 MHz, DMSO-*d6*) δ 8.70 (s, 1H), 8.69 (s, 1H), 8.38 (s, 1H), 7.98 (d, J

= 7.6 Hz, 2H), 7.57 (t, *J* = 7.6 Hz, 2H), 7.49 (t, *J* = 7.6 Hz, 1H), 7.40 (d, *J* = 8.4 Hz, 2H), 7.28 (s, 1H), 7.26 (brs, 1H), 7.23 (d, *J* = 7.9 Hz, 1H), 7.18 (d, *J* = 8.4 Hz, 2H), 7.16 (t, *J* = 7.9 Hz, 1H), 6.75 (d, *J* = 7.9 Hz, 1H), 3.75 (q, *J* = 7.9 Hz, 2H), 2.89 (t, *J* = 7.9 Hz, 2H), 2.40 (d, *J* = 6.8 Hz, 2H), 1.85-1.77 (m, 1H), 0.87 (d, *J* = 6.8 Hz, 6H); ^{13}C NMR (100 MHz, DMSO-*d6*) δ 163.41, 156.40, 154.85, 152.54, 144.02, 141.68, 139.53, 137.92, 132.50, 129.26, 129.04, 128.98, 128.42, 127.60, 125.58, 122.48, 118.63, 118.35, 115.65, 104.46, 100.55, 44.79, 42.23, 34.20, 29.62, 22.17; LCMS (ESI) *m/z*: 540.3 $[M+H]^+$; HRMS (ESI) calcd for $C_{31}H_{30}ClN_5O_2$ $[M+H]^+$ m/z 540.2166; found: 540.2173; HPLC purity = 98.2%, *t*R = 49.37 min.

*4.4.11. 1-(4-(2-((5-chloro-6-phenylfuro[2,3-d]pyrimidin-4-yl)amino)ethyl)phenyl)-3-(3-((dimethylamino)methyl)phenyl)urea (**3m**)*

Following the similar reaction and workup procedures for **3b**, the residue was purified by silica gel column chromatography with MeOH/DCM (5:95) to give **3m**. Yield: 60%; ^{1}H NMR (400 MHz, $CDCl_3$) δ 8.40 (s, 1H), 7.99 (d, *J* = 7.2 Hz, 2H), 7.45 (t, *J* = 7.2 Hz, 2H), 7.38 (t, *J* = 7.2 Hz, 1H), 7.33-7.30 (m, 3H), 7.27-7.26 (m, 2H), 7.24 (s, 1H), 7.20 (d, *J* = 8.6 Hz, 2H), 7.03-6.99 (m, 2H), 5.88 (brs, 1H), 3.85 (q, *J* = 6.4 Hz, 2H), 3.36 (s, 2H), 2.95 (t, *J* = 6.4 Hz, 2H), 2.01 (s, 6H); ^{13}C NMR (100 MHz, $CDCl_3$) δ 163.83, 157.29, 155.11, 153.62, 145.62, 140.31, 138.41, 136.97, 134.60, 129.89, 129.39, 129.35,

128.97, 128.31, 126.23, 125.02, 121.67, 121.51, 119.85, 104.52, 101.79, 64.33, 45.46, 42.41, 35.13 ; LCMS (ESI) *m/z*: 541.3 $[M+H]^+$; HRMS (ESI) calcd for $C_{30}H_{29}ClN_6O_2$ $[M+H]^+$ m/z 541.2119; found: 541.2120; HPLC purity = 98.7%, *t*R = 27.29 min.

*4.4.12. 1-(4-(2-((5-chloro-6-phenylfuro[2,3-d]pyrimidin-4-yl)amino)ethyl)phenyl)-3-(3-((ethyl(methyl)amino)methyl)phenyl)urea (**3n**)*

Following the similar reaction and workup procedures for **3b**, the residue was purified by silica gel column chromatography with MeOH/DCM (5:95) to give **3n**. Yield: 54%; ^{1}H NMR (400 MHz, $CDCl_3$) δ 8.59 (brs, 1H), 8.39 (s, 1H), 8.29 (brs, 1H), 8.01 (d, *J* = 8.0 Hz, 2H), 7.60 (d, *J* = 7.6 Hz, 1H), 7.50-7.44 (m, 5H), 7.40-7.36 (m, 1H), 7.21-7.16 (m, 3H), 6.92 (d, *J* = 7.6 Hz, 1H), 5.89 (brs, 1H), 3.84 (q, *J* = 6.6 Hz, 2H), 3.79 (s, 2H), 2.94 (t, *J* = 6.6 Hz, 2H), 2.87 (q, *J* = 7.2 Hz, 2H), 2.47 (s, 3H), 1.29 (t, *J* = 7.2 Hz, 3H); ^{13}C NMR (100 MHz, DMSO-*d6*) δ 163.44, 156.41, 154.87, 152.66, 144.05, 140.25×2, 137.96, 132.48, 129.32, 129.09, 128.99, 127.59, 125.63×2, 123.71, 119.82, 118.40, 118.16, 104.46, 100.54, 58.69, 49.99, 42.21, 38.89, 34.20, 9.66; LCMS (ESI) *m/z*: 555.2 $[M+H]^+$; HRMS (ESI) calcd for $C_{31}H_{31}ClN_6O_2$ $[M+H]^+$ m/z 555.2275; found: 555.2272; HPLC purity = 97.8%, *t*R = 27.39 min.

*4.4.13. 1-(4-(2-((5-chloro-6-phenylfuro[2,3-d]pyrimidin-4-yl)amino)ethyl)phenyl)-3-(3-((diethylamino)methyl)phenyl)urea (**3o**)*

Following the similar reaction and workup procedures for **3b**, the residue was purified by silica gel column chromatography with MeOH/DCM (5:95) to give **3o**. Yield: 52%; ^{1}H NMR (400 MHz, DMSO-*d6*) δ 8.80 (brs, 1H), 8.71 (brs, 1H), 8.38 (s, 1H), 7.99 (d, *J* = 7.2 Hz, 2H), 7.57 (t, *J* = 7.2 Hz, 2H), 7.87 (t, *J* = 7.2 Hz, 1H), 7.41 (s, 1H), 7.40 (d, *J* = 8.4 Hz, 2H), 7.33 (d, *J* = 7.6 Hz, 1H), 7.27 (brs, 1H), 7.18 (d, *J* = 8.4 Hz, 2H), 7.18 (t, *J* = 7.6 Hz, 1H), 6.89 (d, *J* = 7.6 Hz, 1H), 3.75 (q, *J* = 8.0 Hz, 2H), 3.47 (s, 2H), 2.89 (t, *J* = 8.0 Hz, 2H), 2.45 (q, *J* = 7.2 Hz, 4H), 0.98 (t, *J* = 7.2 Hz, 6H); ^{13}C NMR (100 MHz, DMSO-*d6*) δ 163.44, 156.42, 154.90, 152.53, 144.05, 140.65, 139.66, 137.93, 132.53, 129.31, 129.09, 129.01, 128.43, 127.62, 125.62, 121.98, 118.37, 118.12, 116.48, 104.48, 100.56, 57.02, 46.14, 42.26, 34.22, 11.68; LCMS (ESI) *m/z*: 569.4 $[M+H]^+$; HRMS (ESI) calcd for $C_{32}H_{33}ClN_6O_2$ $[M+H]^+$ m/z 569.2432; found: 569.2425; HPLC purity = 98.8%, *t*R = 27.83 min.

*4.4.14. 1-(4-(2-((5-chloro-6-phenylfuro[2,3-d]pyrimidin-4-yl)amino)ethyl)phenyl)-3-(3-(piperidin-1-ylmethyl)phenyl)urea (**3p**)*

Following the similar reaction and workup procedures for **3b**, the residue was purified by silica gel column chromatography with MeOH/DCM (5:95) to give **3p**. Yield: 21%; ^{1}H NMR (400 MHz, DMSO-*d6*) δ 8.65 (s, 1H), 8.57 (s, 1H), 8.38 (s, 1H), 7.99 (d, *J* = 7.2 Hz, 2H), 7.57 (t, *J* = 7.2 Hz, 2H), 7.49 (t, *J* = 7.2 Hz, 1H), 7.40-7.38 (m, 3H), 7.32

(d, *J* = 8.0 Hz, 1H), 7.28 (br, 1H), 7.22-7.17 (m, 3H), 6.87 (d, *J* = 8.0 Hz, 1H), 3.75 (q, *J* = 7.6 Hz, 2H), 3.38 (s, 2H), 2.89 (t, *J* = 7.6 Hz, 2H), 2.36-2.28 (m, 4H), 1.50-1.48 (m, 4H), 1.42-1.36 (m, 2H); ^{13}C NMR (100 MHz, DMSO-*d6*) δ 163.48, 156.46, 154.93, 152.60, 144.09, 139.78, 137.96×2, 132.55, 129.36, 129.14, 129.03, 128.56, 127.63, 125.66, 122.54, 118.64, 118.39, 116.95, 104.50, 100.59, 62.61, 53.72, 42.27, 34.23, 25.24, 23.75; LCMS (ESI) *m/z*: 581.4 $[M+H]^+$; HRMS (ESI) calcd for $C_{33}H_{33}ClN_6O_2$ $[M+H]^+$ m/z 581.2432; found: 581.2433; HPLC purity = 97.6%, *t*R = 28.19 min.

*4.4.15. 1-(4-(2-((5-chloro-6-phenylfuro[2,3-d]pyrimidin-4-yl)amino)ethyl)phenyl)-3-(3-((4-hydroxypiperidin-1-yl)methyl)phenyl)urea (**3q**)*

Following the similar reaction and workup procedures for **3b**, the residue was purified by silica gel column chromatography with MeOH/DCM (10:90) to give **3q**. Yield: 25%; ^{1}H NMR (400 MHz, DMSO-*d6*) δ 8.73 (s, 1H), 8.65 (s, 1H), 8.38 (s, 1H), 7.98 (d, *J* = 7.6 Hz, 2H), 7.57 (t, *J* = 7.6 Hz, 2H), 7.49 (t, *J* = 7.6 Hz, 1H), 7.41-7.38 (m, 3H), 7.32 (d, *J* = 8.4 Hz, 1H), 7.27 (brs, 1H), 7.20 (d, *J* = 7.6 Hz, 1H), 7.18 (d, *J* = 8.4 Hz, 2H), 6.86 (d, *J* = 7.6 Hz, 1H), 4.53 (d, *J* = 4.0 Hz, 1H), 3.75 (q, *J* = 8.2 Hz, 2H), 3.48-3.40 (m, 1H), 3.78 (s, 2H), 2.89 (t, *J* = 8.2 Hz, 2H), 2.67-2.64 (m, 2H), 2.03-1.98 (m, 2H), 1.71-1.68 (m, 2H), 1.42-1.33 (m, 2H); ^{13}C NMR (100 MHz, DMSO-*d6*) δ 163.44, 156.42, 154.90, 152.53, 144.04, 139.69, 139.37, 137.92, 132.53, 129.32, 129.09, 129.00,

128.48, 127.62, 125.63, 122.20, 118.37, 118.30, 116.66, 104.47, 100.56, 66.37, 62.24, 50.93, 42.25, 34.45, 34.21; LCMS (ESI) *m/z*: 597.3 $[M+H]^+$; HRMS (ESI) calcd for $C_{33}H_{33}ClN_6O_3$ $[M+H]^+$ m/z 597.2381; found: 597.2375; HPLC purity = 99.2%, *t*R = 25.73 min.

*4.4.16. 1-(4-(2-((5-chloro-6-phenylfuro[2,3-d]pyrimidin-4-yl)amino)ethyl)phenyl)-3-(p-tolyl) urea (**3r**)*

Following the similar reaction and workup procedures for **3a**, the residue was purified by silica gel column chromatography with MeOH/DCM (2:98) to give **3r**. Yield: 45%; ^{1}H NMR (400 MHz, $CDCl_3$) δ 8.41 (s, 1H), 8.02 (d, *J* = 7.6 Hz, 2H), 7.48 (t, *J* = 7.6 Hz, 2H), 7.40 (t, *J* = 7.6 Hz, 1H), 7.34 (d, *J* = 8.4 Hz, 2H), 7.24 (d, *J* = 8.4 Hz, 2H), 7.23 (d, *J* = 8.4 Hz, 2H), 7.16 (d, *J* = 8.4 Hz, 2H), 6.48 (s, 1H), 6.38 (s, 1H), 5.89 (brs, 1H), 3.88 (q, *J* = 6.8 Hz, 2H), 2.98 (t, *J* = 6.8 Hz, 2H), 2.34 (s, 3H); ^{13}C NMR (100 MHz, DMSO-*d6*) δ 163.45, 156.42, 154.91, 152.59, 144.05, 138.00, 137.18, 132.44, 130.54, 129.33, 129.16, 129.11, 129.00, 127.62, 125.64, 118.31, 118.22, 104.48, 100.56, 42.26, 34.21, 20.34; LCMS (ESI) *m/z*: 498.2 $[M+H]^+$; HRMS (ESI) calcd for $C_{28}H_{24}ClN_5O_2$ $[M+H]^+$ m/z 498.1697; found: 498.1711; HPLC purity = 99.8%, *t*R = 44.51 min.

*4.4.17. 1-(4-(2-((5-chloro-6-phenylfuro[2,3-d]pyrimidin-4-yl)amino)ethyl)phenyl)-3-(4-ethylphenyl)urea (**3s**)*

Following the similar reaction and workup procedures for **3a**, the residue was purified by silica gel column chromatography with MeOH/DCM (2:98) to give **3s**. Yield: 60%; ^{1}H NMR (400 MHz, DMSO-*d6*) δ 8.59 (s, 1H), 8.56 (s, 1H), 8.37 (s, 1H), 7.98 (d, *J* = 7.6 Hz, 2H), 7.57 (t, *J* = 7.6 Hz, 2H), 7.48 (t, *J* = 7.6 Hz, 1H), 7.38 (d, *J* = 7.8 Hz, 2H), 7.34 (d, *J* = 7.8 Hz, 2H), 7.27 (brs, 1H), 7.18 (d, *J* = 7.8 Hz, 2H), 7.10 (d, *J* = 7.8 Hz, 2H), 3.75 (q, *J* = 7.2 Hz, 2H), 2.88 (t, *J* = 7.2 Hz, 2H), 2.56-2.52 (m, 2H), 1.15 (t, *J* = 7.6 Hz, 3H); ^{13}C NMR (100 MHz, DMSO-*d6*) δ 163.47, 156.45, 154.92, 152.63, 144.09, 138.01, 137.38, 137.14, 132.47, 129.37, 129.13×2, 129.02, 127.63, 125.66, 118.34×2, 104.50, 100.58, 42.26, 34.23, 27.53, 15.83; LCMS (ESI) *m/z*: 512.3 $[M+H]^+$; HRMS (ESI) calcd for $C_{29}H_{26}ClN_5O_2$ $[M+H]^+$ m/z 512.1853; found: 512.1868; HPLC purity = 97.6%, *t*R = 46.64 min.

*4.4.17. 1-(4-(2-((5-chloro-6-phenylfuro[2,3-d]pyrimidin-4-yl)amino)ethyl)phenyl)-3-(4-isopropylphenyl)urea (**3t**)*

Following the similar reaction and workup procedures for **3a**, the residue was purified by silica gel column chromatography with MeOH/DCM (2:98) to give **3t**. Yield: 40%; ^{1}H NMR (400 MHz, DMSO-*d6*) δ 8.56 (s, 1H), 8.53 (s, 1H), 8.37 (s, 1H), 7.98 (d, *J* = 7.2 Hz, 2H), 7.57 (t, *J* = 7.2 Hz, 2H), 7.48 (t, *J* = 7.2 Hz, 1H), 7.39 (d, *J* = 8.4 Hz, 2H), 7.34 (d, *J* = 8.4 Hz, 2H), 7.26 (brs, 1H), 7.18 (d, *J* = 8.4 Hz, 2H), 7.13 (d, *J* = 8.4 Hz, 2H),

3.75 (q, *J* = 8.0 Hz, 2H), 2.88 (t, *J* = 8.0 Hz, 2H), 2.82 (sep, *J* = 7.0 Hz, 1H), 1.17 (d, *J* = 7.0 Hz, 6H); ^{13}C NMR (100 MHz, DMSO-*d6*) δ 163.44, 156.42, 154.89, 152.62, 144.04, 141.78, 138.02, 137.45, 132.41, 129.31, 129.08, 128.98, 127.61, 126.45, 125.62, 118.33, 118.30, 104.47, 100.56, 42.24, 34.20, 32.76, 24.02; LCMS (ESI) *m/z*: 526.3 $[M+H]^+$; HRMS (ESI) calcd for $C_{30}H_{28}ClN_5O_2$ $[M+H]^+$ m/z 526.2010; found: 526.2026; HPLC purity = 99.4%, *t*R = 47.78 min.

*4.4.18. 1-(4-(2-((5-chloro-6-phenylfuro[2,3-d]pyrimidin-4-yl)amino)ethyl)phenyl)-3-(4-isobutylphenyl)urea (**3u**)*

Following the similar reaction and workup procedures for **3b**, the residue was purified by silica gel column chromatography with MeOH/DCM (2:98) to give **3u**. Yield: 63%; ^{1}H NMR (400 MHz, DMSO-*d6*) δ 8.55 (s, 1H), 8.52 (s, 1H), 8.37 (s, 1H), 7.98 (d, *J* = 7.6 Hz, 2H), 7.57 (t, *J* = 7.6 Hz, 2H), 7.48 (t, *J* = 7.6 Hz, 1H), 7.38 (d, *J* = 8.0 Hz, 2H), 7.33 (d, *J* = 8.0 Hz, 2H), 7.27 (brs, 1H), 7.18 (d, *J* = 8.0 Hz, 2H), 7.05 (d, *J* = 8.0 Hz, 2H), 3.75 (q, *J* = 6.8 Hz, 2H), 2.88 (t, *J* = 6.8 Hz, 2H), 2.37 (d, *J* = 6.8 Hz, 2H), 1.82-1.74 (m, 1H), 0.85 (d, *J* = 6.8 Hz, 6H); ^{13}C NMR (100 MHz, DMSO-*d6*) δ 163.48, 156.46, 154.94, 152.63, 144.10, 138.02, 137.44, 134.49, 132.40, 129.39, 129.20, 129.16, 129.04, 127.64, 125.68, 118.34, 118.15, 104.51, 100.59, 44.02, 42.28, 34.23, 29.76, 22.16; LCMS (ESI) *m/z*: 540.3 $[M+H]^+$; HRMS (ESI) calcd for $C_{31}H_{30}ClN_5O_2$ $[M+H]^+$ m/z 540.2166; found:

540.2172; HPLC purity = 99.7%, *t*R = 49.41 min.

*4.4.19. 1-(4-(2-((5-chloro-6-phenylfuro[2,3-d]pyrimidin-4-yl)amino)ethyl)phenyl)-3-(4-((dimethylamino)methyl)phenyl)urea (**3v**)*

Following the similar reaction and workup procedures for **3b**, the residue was purified by silica gel column chromatography with MeOH/DCM (5:95) to give **3v**. Yield: 57%; ^{1}H NMR (400 MHz, DMSO-*d6*) δ 8.61 (s, 1H), 8.60 (s, 1H), 8.35 (s, 1H), 7.96 (d, *J* = 8.0 Hz, 2H), 7.55 (t, *J* = 8.0 Hz, 2H), 7.46 (t, *J* = 8.0 Hz, 1H), 7.39 (d, *J* = 7.6 Hz, 2H), 7.38 (d, *J* = 7.6 Hz, 2H), 7.29-7.14 (m, 5H), 3.74 (q, *J* = 7.6 Hz, 2H), 3.29 (s, 2H), 2.88 (t, *J* = 7.6 Hz, 2H), 2.10 (s, 6H); ^{13}C NMR (100 MHz, DMSO-*d6*) δ 163.48, 156.48, 154.91, 152.63, 144.11, 138.54, 137.98, 132.55, 132.17, 129.37, 129.26, 129.13, 129.04, 127.64, 125.67, 118.42, 117.99, 104.51, 100.60, 63.00, 44.86, 42.26, 34.23; LCMS (ESI) *m/z*: 541.3 $[M+H]^+$; HRMS (ESI) calcd for $C_{30}H_{29}ClN_6O_2$ $[M+H]^+$ m/z 541.2119; found: 541.2126; HPLC purity = 91.8%, *t*R = 26.43 min.

*4.4.20. 1-(4-(2-((5-chloro-6-phenylfuro[2,3-d]pyrimidin-4-yl)amino)ethyl)phenyl)-3-(4-((diethylamino)methyl)phenyl)urea (**3w**)*

Following the similar reaction and workup procedures for **3b**, the residue was purified by silica gel column chromatography with MeOH/DCM (5:95) to give **3w**. Yield: 47%; ^{1}H NMR (400 MHz, $CDCl_3$) δ 8.41 (s, 1H), 8.02 (d, *J* = 7.2 Hz, 2H), 7.52-7.44 (m,

7H), 7.44-7.38 (m, 3H), 7.21 (d, *J* = 8.4 Hz, 2H), 5.90 (brs, 1H), 3.88 (q, *J* = 6.8 Hz, 2H), 3.83 (s, 2H), 2.97 (t, *J* = 6.8 Hz, 2H), 2.86 (q, *J* = 6.8 Hz, 4H), 1.25 (d, *J* = 6.8 Hz, 6H); ^{13}C NMR (100 MHz, DMSO-*d6*) δ 163.41, 156.39, 154.86, 152.65, 144.00, 139.73, 137.99, 132.46, 130.36, 129.26, 129.04×2, 128.99, 127.60, 125.58, 118.21, 117.82, 104.47, 100.55, 55.44, 45.72, 42.23, 34.21, 10.03; LCMS (ESI) *m/z*: 569.3 $[M+H]^+$; HRMS (ESI) calcd for $C_{32}H_{33}ClN_6O_2$ $[M+H]^+$ m/z 569.2432; found: 569.2444; HPLC purity = 95.6%, *t*R = 26.43 min.

*4.4.21. 1-(4-(2-((5-chloro-6-phenylfuro[2,3-d]pyrimidin-4-yl)amino)ethyl)phenyl)-3-(4-(piperidin-1-ylmethyl)phenyl)urea (**3x**)*

Following the similar reaction and workup procedures for **3b**, the residue was purified by silica gel column chromatography with MeOH/DCM (5:95) to give **3x**. Yield: 36%; ^{1}H NMR (400 MHz, DMSO-*d6*) δ 9.26 (brs, 1H), 9.07 (brs, 1H), 8.37 (s, 1H), 7.98 (d, *J* = 8.0 Hz, 2H), 7.57 (t, *J* = 8.0 Hz, 2H), 7.52 (d, *J* = 8.4 Hz, 2H), 7.48 (t, *J* = 8.0 Hz, 1H), 7.42 (d, *J* = 8.4 Hz, 2H), 7.40 (d, *J* = 8.4 Hz, 2H), 7.26 (brs, 1H), 7.19 (d, *J* = 8.4 Hz, 2H), 4.20-4.12 (m, 2H), 3.75 (q, *J* = 7.6 Hz, 2H), 3.29-3.25 (m, 2H), 2.89 (t, *J* = 7.6 Hz, 2H), 2.85-2.76 (m, 2H), 1.82-1.63 (m, 6H); ^{13}C NMR (100 MHz, DMSO-*d6*) δ 163.43, 156.41, 154.88, 152.64, 144.04, 141.04, 137.91, 132.54, 132.07, 129.31, 129.08×2, 129.00, 127.60, 125.62, 118.20, 117.67, 104.67, 100.55, 58.74, 51.40, 42.22, 34.21, 22.26,

21.45; LCMS (ESI) *m/z*: 581.3 $[M+H]^+$; HRMS (ESI) calcd for $C_{33}H_{33}ClN_6O_2$ $[M+H]^+$ m/z 581.2432; found: 581.2435; HPLC purity = 97.7%, *t*R = 27.99 min.

*4.4.22. 1-(4-(2-((5-chloro-6-phenylfuro[2,3-d]pyrimidin-4-yl)amino)ethyl)phenyl)-3-(4-((4-hydroxypiperidin-1-yl)methyl)phenyl)urea (**3y**)*

Following the similar reaction and workup procedures for **3b**, the residue was purified by silica gel column chromatography with MeOH/DCM (10:90) to give **3y**. Yield: 21%; ^{1}H NMR (400 MHz, DMSO-*d6*) δ 8.64-8.58 (m, 2H), 8.37 (s, 1H), 7.98 (d, *J* = 7.6 Hz, 2H), 7.57 (t, *J* = 7.6 Hz, 2H), 7.48 (t, *J* = 7.6 Hz, 1H), 7.39 (d, *J* = 8.0 Hz, 2H), 7.37 (d, *J* = 8.0 Hz, 2H), 7.25 (brs, 1H), 7.18 (d, *J* = 8.0 Hz, 2H), 7.16 (d, *J* = 8.0 Hz, 2H), 4.52 (d, *J* = 3.2 Hz, 1H), 3.75 (q, *J* = 7.2 Hz, 2H), 3.48-3.39 (m, 1H), 3.35 (s, 2H), 2.89 (t, *J* = 7.2 Hz, 2H), 2.68-2.60 (m, 2H), 2.03-1.95 (m, 2H), 1.72-1.65 (m, 2H), 1.41-1.32 (m, 2H); ^{13}C NMR (100 MHz, DMSO-*d6*) δ 163.44, 156.43, 154.90, 152.57, 144.05, 138.46, 137.96, 132.48, 131.88, 129.32, 129.24, 129.09, 129.00, 127.62, 125.63, 118.33, 117.96, 104.47, 100.56, 66.46, 61.71, 50.80, 42.25, 34.43, 34.21; LCMS (ESI) *m/z*: 597.3 $[M+H]^+$; HRMS (ESI) calcd for $C_{33}H_{33}ClN_6O_3$ $[M+H]^+$ m/z 597.2381; found: 597.2382; HPLC purity = 97.8%, *t*R = 24.43 min.

4.5. Docking analysis of compounds with Aurora-A and Aurora-B

The human Aurora-B structure (PDB ID: 4AF3) is missing some residues around the

DFG loop [10, 45]. The missing residues in the X-ray structure of Aurora-B were restored using Discovery Studio 2016/*Buil*d homology modeling program (BIOVIA, Inc., San Diego, CA, USA) (Fig. S2, supplementary data). The protein structures of Aurora-A (PDB ID: 2W1C) and the repaired Aurora-B were used for the docking study. The docking analysis was conducted using the Discovery Studio 2016//LigandFit program with the CHARMm force field [46]. The number of docking poses was set as 100 with default parameters. The decision of the best conformation was determined according the complex binding structure from our previous Aurora kinase studies [29, 44, 47, 48].

4.6. Aurora kinase assays.

Inhibitory activities of the compounds against Aurora-A and Aurora-B were measured by Kinase-Glo® Luminescent Kinase Assays as previously described [28, 29]. Briefly, the recombinant GST-tagged human Aurora-A (amino acids 123-401) containing the kinase domain was expressed in Sf9 insect cells and purified by glutathione affinity chromatography. The recombinant full length human Aurora-B (residues 1-344) produced in Sf9 insect cells was obtained from Invitrogen (Invitrogen, USA). The reactions were carried out in 96-well plates in a final volume of 50 μL solution per reaction containing 50 mM Tris-HCl pH 7.4, 10 mM NaCl, 10 mM $MgCl_2$, 0.01% BSA, 5.0 μM ATP, 1 mM DTT, 15 μM tetra(-LRRASLG) peptide, the tested compound, and 150 ng recombinant

Aurora-A or 40 ng recombinant Aurora-B. The plates were incubated at either 37 °C for 120 minutes for Aurora-A or at 30 °C for 90 min for Aurora-B). Then, Kinase-Glo Plus Reagent (50 μL; Promega, USA) was added, and the mixture was incubated at 25 °C for 20 minutes. A 70 μL aliquot of each reaction mixture was transferred to a black microliter plate, and luminescence was measured on a Wallac Vector 1420 multilabel counter (PerkinElmer, USA).

4.7. Cell culture

Human colorectal cancer HCT116 and human cervical cancer HeLa cells were maintained in high glucose Dulbecco's Modified Eagle Medium (DMEM, Invitrogen, USA) supplemented with 10% fetal bovine serum (FBS, Biological Industries, USA), 2 mM L-glutamine and antibiotics. Human normal skin fibroblasts Detroit 551 (ATCC, USA) were maintained in high glucose Eagle's Minimum Essential Medium (MEM, Invitrogen, USA) supplemented with 10% FBS, 2 mM L-glutamine and antibiotics.

4.8. Western blot

HCT116 cells were first synchronized in mitosis by 200 nM nocodazole treatment for 24 hours. After one hour of compound treatment, cells were washed with 1× phosphate buffered saline (PBS) and then lysed in 1× Laemmli protein sample buffer and boiling at 100 ^{o}C for 10 minutes. Lysates were analyzed by SDS-PAGE, transferred to

polyvinylidene fluoride (PVDF, Millipore, USA) membrane and blotted with antibodies. For Western blotting of phosphorylated Aurora-A (Thr288)/Aurora-B (Thr232)/Aurora-C(Thr198), the antibody (Cell Signaling, USA) was diluted in 5% BSA (bovine serum albumin, Sigma-Aldrich, USA). After washes with 1× TBST (Tris-buffer saline + 0.1 % Tween-20), horseradish peroxidase (HRP)-conjugated secondary antibodies (Sigma-Aldrich, USA) were added, and the blots were developed by chemiluminescence.

4.9. Immunofluorescence staining

Cells were fixed in 4% paraformaldehyde in PBS for 30 minutes and permeabilized with 0.1% TritonX-100 for 10 minutes at room temperature. Cells were incubated with 1% BSA in PBS for 30 minutes to block nonspecific binding. An antibody specific to phosphorylated histone H3 at serine 10 (pHH3Ser10, Abcam, UK) was added at a dilution of 1:500 and incubated for 1.5 hours at room temperature. After three washes with PBS, cells were probed with an Alexa-594-conjugated secondary antibody (Invitrogen, USA). Cell nuclei were counterstained with Hoechst 33342 (Invitrogen, USA). Immunofluorescence signals were visualized using a Leica microscope (DM2500, Leica, Germany) equipped with an Olympus CCD (DP73, Olympus, Japan). Images were processed by MetaMorph software (Molecular Devices, USA) for the quantifying number of cells stained positive for pHH3Ser10.

Conflict of interest

The authors declare no competing financial interest.

Acknowledgement

Financial support from the National Health Research Institutes and Ministry of Science and Technology, Taiwan (MOST-105-0324-01-13-06 and MOST-106-2113-M-400-001) are gratefully acknowledged. We thank Core Instrument Center of NHRI to provide fluorescence microscopy service.

Appendix A. Supplementary data

Figure S1. Protein sequence alignment of Aurora-A (2W1C) and Aurora-B (4AF3) in the X-ray structure.

Figure S2. Repair of the missing residues of Aurora-B in the X-ray structure (PDB ID: 4AF3) using homology modeling

Figure S3. ^{1}H and ^{13}C spectra of the synthesized compounds in Table 1.

References

[1] M. Carmena, W.C. Earnshaw, The cellular geography of aurora kinases, Nat Rev Mol Cell Biol, 4 (2003) 842-854.

[2] S.M. Lens, E.E. Voest, R.H. Medema, Shared and separate functions of polo-like kinases and aurora kinases in cancer, Nat Rev Cancer, 10 (2010) 825-841.

[3] J. Fu, M. Bian, Q. Jiang, C. Zhang, Roles of Aurora kinases in mitosis and tumorigenesis, Mol Cancer Res, 5 (2007) 1-10.

[4] V. Agnese, V. Bazan, F.P. Fiorentino, D. Fanale, G. Badalamenti, G. Colucci, V. Adamo, D. Santini, A. Russo, The role of Aurora-A inhibitors in cancer therapy, Ann Oncol, 18 Suppl 6 (2007) vi47-52.

[5] M. Tatsuka, H. Katayama, T. Ota, T. Tanaka, S. Odashima, F. Suzuki, Y. Terada, Multinuclearity and increased ploidy caused by overexpression of the aurora- and Ipl1-like midbody-associated protein mitotic kinase in human cancer cells, Cancer Res, 58 (1998) 4811-4816.

[6] M. Kollareddy, D. Zheleva, P. Dzubak, P.S. Brahmkshatriya, M. Lepsik, M. Hajduch, Aurora kinase inhibitors: progress towards the clinic, Invest New Drugs, 30 (2012) 2411-2432.

[7] S. Anand, S. Penrhyn-Lowe, A.R. Venkitaraman, Aurora-A amplification overrides the mitotic spindle assembly checkpoint, inducing resistance to Taxol, Cancer Cell, 3 (2003) 51-62.

[8] D.M. Glover, M.H. Leibowitz, D.A. McLean, H. Parry, Mutations in aurora prevent centrosome separation leading to the formation of monopolar spindles, Cell, 81 (1995) 95-105.

[9] Y. Terada, Y. Uetake, R. Kuriyama, Interaction of Aurora-A and centrosomin at the microtubule-nucleating site in Drosophila and mammalian cells, J Cell Biol, 162 (2003) 757-763.

[10] J.M. Elkins, S. Santaguida, A. Musacchio, S. Knapp, Crystal structure of human aurora B in complex with INCENP and VX-680, J Med Chem, 55 (2012) 7841-7848.

[11] S. Ruchaud, M. Carmena, W.C. Earnshaw, Chromosomal passengers: conducting cell division, Nat Rev Mol Cell Biol, 8 (2007) 798-812.

[12] R.R. Adams, S.P. Wheatley, A.M. Gouldsworthy, S.E. Kandels-Lewis, M. Carmena, C. Smythe, D.L. Gerloff, W.C. Earnshaw, INCENP binds the Aurora-related kinase AIRK2 and is required to target it to chromosomes, the central spindle and cleavage furrow, Curr Biol, 10 (2000) 1075-1078.

[13] T.U. Tanaka, N. Rachidi, C. Janke, G. Pereira, M. Galova, E. Schiebel, M.J. Stark, K.

Nasmyth, Evidence that the Ipl1-Sli15 (Aurora kinase-INCENP) complex promotes chromosome bi-orientation by altering kinetochore-spindle pole connections, Cell, 108 (2002) 317-329.

[14] S. Kaitna, M. Mendoza, V. Jantsch-Plunger, M. Glotzer, Incenp and an Aurora-like kinase form a complex essential for chromosome segregation and efficient completion of cytokinesis, Curr Biol, 10 (2000) 1172-1181.

[15] S.G. Zeitlin, R.D. Shelby, K.F. Sullivan, CENP-A is phosphorylated by Aurora B kinase and plays an unexpected role in completion of cytokinesis, J Cell Biol, 155 (2001) 1147-1157.

[16] A.G. Uren, L. Wong, M. Pakusch, K.J. Fowler, F.J. Burrows, D.L. Vaux, K.H. Choo, Survivin and the inner centromere protein INCENP show similar cell-cycle localization and gene knockout phenotype, Curr Biol, 10 (2000) 1319-1328.

[17] K.K. Hanson, A.C. Kelley, M. Bienz, Loss of Drosophila borealin causes polyploidy, delayed apoptosis and abnormal tissue development, Development, 132 (2005) 4777-4787.

[18] R.W. Wilkinson, R. Odedra, S.P. Heaton, S.R. Wedge, N.J. Keen, C. Crafter, J.R. Foster, M.C. Brady, A. Bigley, E. Brown, K.F. Byth, N.C. Barrass, K.E. Mundt, K.M. Foote, N.M. Heron, F.H. Jung, A.A. Mortlock, F.T. Boyle, S. Green, AZD1152, a selective inhibitor of Aurora B kinase, inhibits human tumor xenograft growth by inducing apoptosis, Clin Cancer Res, 13 (2007) 3682-3688.

[19] E.A. Harrington, D. Bebbington, J. Moore, R.K. Rasmussen, A.O. Ajose-Adeogun, T. Nakayama, J.A. Graham, C. Demur, T. Hercend, A. Diu-Hercend, M. Su, J.M. Golec, K.M. Miller, VX-680, a potent and selective small-molecule inhibitor of the Aurora kinases, suppresses tumor growth in vivo, Nat Med, 10 (2004) 262-267.

[20] M.G. Manfredi, J.A. Ecsedy, K.A. Meetze, S.K. Balani, O. Burenkova, W. Chen, K.M. Galvin, K.M. Hoar, J.J. Huck, P.J. LeRoy, E.T. Ray, T.B. Sells, B. Stringer, S.G. Stroud, T.J. Vos, G.S. Weatherhead, D.R. Wysong, M. Zhang, J.B. Bolen, C.F. Claiborne, Antitumor activity of MLN8054, an orally active small-molecule inhibitor of Aurora A kinase, Proc Natl Acad Sci U S A, 104 (2007) 4106-4111.

[21] H. Katayama, S. Sen, Aurora kinase inhibitors as anticancer molecules, Biochim Biophys Acta, 1799 (2010) 829-839.

[22] G. Gorgun, E. Calabrese, T. Hideshima, J. Ecsedy, G. Perrone, M. Mani, H. Ikeda, G. Bianchi, Y. Hu, D. Cirstea, L. Santo, Y.T. Tai, S. Nahar, M. Zheng, M. Bandi, R.D. Carrasco, N. Raje, N. Munshi, P. Richardson, K.C. Anderson, A novel Aurora-A kinase inhibitor MLN8237 induces cytotoxicity and cell-cycle arrest in multiple myeloma, Blood, 115 (2010) 5202-5213.

[23] N. Keen, S. Taylor, Aurora-kinase inhibitors as anticancer agents, Nat Rev Cancer, 4 (2004) 927-936.
[24] J.F. Seymour, D.W. Kim, E. Rubin, A. Haregewoin, J. Clark, P. Watson, T. Hughes, I. Dufva, J.L. Jimenez, F.X. Mahon, P. Rousselot, J. Cortes, G. Martinelli, C. Papayannidis, A. Nagler, F.J. Giles, A phase 2 study of MK-0457 in patients with BCR-ABL T315I mutant chronic myelogenous leukemia and philadelphia chromosome-positive acute lymphoblastic leukemia, Blood Cancer J, 4 (2014) e238.
[25] C.H. Cheung, S. Sarvagalla, J.Y. Lee, Y.C. Huang, M.S. Coumar, Aurora kinase inhibitor patents and agents in clinical testing: an update (2011 - 2013), Expert Opin Ther Pat, 24 (2014) 1021-1038.
[26] T.B. Sells, R. Chau, J.A. Ecsedy, R.E. Gershman, K. Hoar, J. Huck, D.A. Janowick, V.J. Kadambi, P.J. LeRoy, M. Stirling, S.G. Stroud, T.J. Vos, G.S. Weatherhead, D.R. Wysong, M. Zhang, S.K. Balani, J.B. Bolen, M.G. Manfredi, C.F. Claiborne, MLN8054 and Alisertib (MLN8237): discovery of selective oral Aurora A inhibitors, ACS Med Chem Lett, 6 (2015) 630-634.
[27] V. Bavetsias, S. Linardopoulos, Aurora kinase inhibitors: current status and outlook, Front Oncol, 5 (2015) 278.
[28] C.H. Cheung, W.H. Lin, J.T. Hsu, T.C. Hour, T.K. Yeh, S. Ko, T.W. Lien, M.S. Coumar, J.F. Liu, W.Y. Lai, H.Y. Shiao, T.R. Lee, H.P. Hsieh, J.Y. Chang, BPR1K653, a novel Aurora kinase inhibitor, exhibits potent anti-proliferative activity in MDR1 (P-gp170)-mediated multidrug-resistant cancer cells, PLoS One, 6 (2011) e23485.
[29] H.Y. Shiao, M.S. Coumar, C.W. Chang, Y.Y. Ke, Y.H. Chi, C.Y. Chu, H.Y. Sun, C.H. Chen, W.H. Lin, K.S. Fung, P.C. Kuo, C.T. Huang, K.Y. Chang, C.T. Lu, J.T. Hsu, C.T. Chen, W.T. Jiaang, Y.S. Chao, H.P. Hsieh, Optimization of ligand and lipophilic efficiency to identify an in vivo active furano-pyrimidine Aurora kinase inhibitor, J Med Chem, 56 (2013) 5247-5260.
[30] Y.H. Peng, H.Y. Shiao, C.H. Tu, P.M. Liu, J.T. Hsu, P.K. Amancha, J.S. Wu, M.S. Coumar, C.H. Chen, S.Y. Wang, W.H. Lin, H.Y. Sun, Y.S. Chao, P.C. Lyu, H.P. Hsieh, S.Y. Wu, Protein kinase inhibitor design by targeting the Asp-Phe-Gly (DFG) motif: the role of the DFG motif in the design of epidermal growth factor receptor inhibitors, J Med Chem, 56 (2013) 3889-3903.
[31] Y. Yasui, T. Urano, A. Kawajiri, K. Nagata, M. Tatsuka, H. Saya, K. Furukawa, T. Takahashi, I. Izawa, M. Inagaki, Autophosphorylation of a newly identified site of Aurora-B is indispensable for cytokinesis, J Biol Chem, 279 (2004) 12997-13003.
[32] P.A. Eyers, E. Erikson, L.G. Chen, J.L. Maller, A novel mechanism for activation of the protein kinase Aurora A, Curr Biol, 13 (2003) 691-697.

[33] S.K. Chiou, N. Hoa, A. Hodges, L. Ge, M.R. Jadus, Indomethacin promotes apoptosis in gastric cancer cells through concomitant degradation of Survivin and Aurora B kinase proteins, Apoptosis, 19 (2014) 1378-1388.
[34] J. Li, M.G. Anderson, L.A. Tucker, Y. Shen, K.B. Glaser, O.J. Shah, Inhibition of Aurora B kinase sensitizes a subset of human glioma cells to TRAIL concomitant with induction of TRAIL-R2, Cell Death Differ, 16 (2009) 498-511.
[35] M.J. Yoon, S.S. Park, Y.J. Kang, I.Y. Kim, J.A. Lee, J.S. Lee, E.G. Kim, C.W. Lee, K.S. Choi, Aurora B confers cancer cell resistance to TRAIL-induced apoptosis via phosphorylation of survivin, Carcinogenesis, 33 (2012) 492-500.
[36] J.J. Yu, L.D. Zhou, T.T. Zhao, W. Bai, J. Zhou, W. Zhang, Knockdown of Aurora-B inhibits the growth of non-small cell lung cancer A549 cells, Oncol Lett, 10 (2015) 1642-1648.
[37] S.J. He, L.P. Shu, Z.W. Zhou, T. Yang, W. Duan, X. Zhang, Z.X. He, S.F. Zhou, Inhibition of Aurora kinases induces apoptosis and autophagy via AURKB/p70S6K/RPL15 axis in human leukemia cells, Cancer Lett, 382 (2016) 215-230.
[38] P. Carpinelli, J. Moll, Aurora kinase inhibitors: identification and preclinical validation of their biomarkers, Expert Opin Ther Targets, 12 (2008) 69-80.
[39] H.T. Ma, R.Y. Poon, Synchronization of HeLa cells, Methods Mol Biol, 761 (2011) 151-161.
[40] S. Sarvagalla, M.S. Coumar, Structural biology insight for the design of sub-type selective Aurora kinase inhibitors, Curr Cancer Drug Targets, 15 (2015) 375-393.
[41] Z. Fang, C. Grutter, D. Rauh, Strategies for the selective regulation of kinases with allosteric modulators: exploiting exclusive structural features, ACS Chem Biol, 8 (2013) 58-70.
[42] A. Pflug, T.M. de Oliveira, D. Bossemeyer, R.A. Engh, Mutants of protein kinase A that mimic the ATP-binding site of Aurora kinase, Biochem J, 440 (2011) 85-93.
[43] V. Bavetsias, A. Faisal, S. Crumpler, N. Brown, M. Kosmopoulou, A. Joshi, B. Atrash, Y. Perez-Fuertes, J.A. Schmitt, K.J. Boxall, R. Burke, C. Sun, S. Avery, K. Bush, A. Henley, F.I. Raynaud, P. Workman, R. Bayliss, S. Linardopoulos, J. Blagg, Aurora isoform selectivity: design and synthesis of imidazo[4,5-b]pyridine derivatives as highly selective inhibitors of Aurora-A kinase in cells, J Med Chem, 56 (2013) 9122-9135.
[44] J.M. Wu, C.T. Chen, M.S. Coumar, W.H. Lin, Z.J. Chen, J.T. Hsu, Y.H. Peng, H.Y. Shiao, W.H. Lin, C.Y. Chu, J.S. Wu, C.T. Lin, C.P. Chen, C.C. Hsueh, K.Y. Chang, L.P. Kao, C.Y. Huang, Y.S. Chao, S.Y. Wu, H.P. Hsieh, Y.H. Chi, Aurora kinase inhibitors reveal mechanisms of HURP in nucleation of centrosomal and kinetochore microtubules, Proc Natl Acad Sci U S A, 110 (2013) E1779-1787.

[45] S. Howard, V. Berdini, J.A. Boulstridge, M.G. Carr, D.M. Cross, J. Curry, L.A. Devine, T.R. Early, L. Fazal, A.L. Gill, M. Heathcote, S. Maman, J.E. Matthews, R.L. McMenamin, E.F. Navarro, M.A. O'Brien, M. O'Reilly, D.C. Rees, M. Reule, D. Tisi, G. Williams, M. Vinkovic, P.G. Wyatt, Fragment-based discovery of the pyrazol-4-yl urea (AT9283), a multitargeted kinase inhibitor with potent aurora kinase activity, J Med Chem, 52 (2009) 379-388.

[46] B.R. Brooks, C.L. Brooks, 3rd, A.D. Mackerell, Jr., L. Nilsson, R.J. Petrella, B. Roux, Y. Won, G. Archontis, C. Bartels, S. Boresch, A. Caflisch, L. Caves, Q. Cui, A.R. Dinner, M. Feig, S. Fischer, J. Gao, M. Hodoscek, W. Im, K. Kuczera, T. Lazaridis, J. Ma, V. Ovchinnikov, E. Paci, R.W. Pastor, C.B. Post, J.Z. Pu, M. Schaefer, B. Tidor, R.M. Venable, H.L. Woodcock, X. Wu, W. Yang, D.M. York, M. Karplus, CHARMM: the biomolecular simulation program, J Comput Chem, 30 (2009) 1545-1614.

[47] M.S. Coumar, J.S. Leou, P. Shukla, J.S. Wu, A.K. Dixit, W.H. Lin, C.Y. Chang, T.W. Lien, U.K. Tan, C.H. Chen, J.T. Hsu, Y.S. Chao, S.Y. Wu, H.P. Hsieh, Structure-based drug design of novel Aurora kinase A inhibitors: structural basis for potency and specificity, J Med Chem, 52 (2009) 1050-1062.

[48] Y.Y. Ke, H.Y. Shiao, Y.C. Hsu, C.Y. Chu, W.C. Wang, Y.C. Lee, W.H. Lin, C.H. Chen, J.T. Hsu, C.W. Chang, C.W. Lin, T.K. Yeh, Y.S. Chao, M.S. Coumar, H.P. Hsieh, 3D-QSAR-assisted drug design: identification of a potent quinazoline-based Aurora kinase inhibitor, ChemMedChem, 8 (2013) 136-148.